Journal of Physics: Condensed Matter



# *In situ* and *operando* electron microscopy in heterogeneous catalysis – Insights into multi-scale chemical dynamics

To cite this article before publication: See Wee Chee *et al* 2021 *J. Phys.: Condens. Matter* in press https://doi.org/10.1088/1361-648X/abddfd

# *In situ* and *Operando* Electron Microscopy in Heterogeneous Catalysis – Insights into Multi-Scale Chemical Dynamics

See Wee Chee*,[1] Thomas Lunkenbein,[2] Robert Schlögl[2,3] and Beatriz Roldan Cuenya[1]

[1] Department of Interface Science, Fritz Haber Institute of the Max Planck Society, 14195 Berlin, Germany

[2] Department of Inorganic Chemistry, Fritz Haber Institute of the Max Planck Society, 14195 Berlin, Germany

[3] Department of Heterogeneous Reactions, Max Planck Institute for Chemical Energy Conversion, 45413 Mülheim an der Ruhr, Germany

* e-mail: swchee@fhi-berlin.mpg.de

**Abstract**

This review features state-of-the-art *in situ* and *operando* electron microscopy (EM) studies of heterogeneous catalysts in gas and liquid environments during reaction. Heterogeneous catalysts are important materials for the efficient production of chemicals/fuels on an industrial scale and for energy conversion applications. They also play a central role in various emerging technologies that are needed to ensure a sustainable future for our society. Currently, the rational design of catalysts has largely been hampered by our lack of insight into the working structures that exist during reaction and their associated properties. However, elucidating the working state of catalysts is not trivial, because catalysts are metastable functional materials that adapt dynamically to a specific reaction condition. The structural or morphological alterations induced by chemical reactions can also vary locally. A complete description of their morphologies requires that the microscopic studies undertaken span several length scales. EMs, especially transmission electron microscopes, are powerful tools for studying the structure of catalysts at the nanoscale because of their high spatial resolution, relatively high temporal resolution, and complementary capabilities for chemical analysis. Furthermore, recent advances have enabled the direct observation of catalysts under realistic environmental conditions using specialized reaction cells. Here, we will critically discuss the importance of spatially-resolved *operando* measurements and the available experimental setups that enable (1) correlated studies where EM observations are complemented by separate measurements of reaction kinetics or spectroscopic analysis of chemical species during reaction or (2) real-time studies where the dynamics of catalysts are followed with EM and the catalytic performance is extracted directly from the reaction cell that is within the EM column or chamber. Examples of current research in this field will be presented. Challenges in the experimental application of these techniques and our perspectives on the field's future directions will also be discussed.

## 1. Introduction

Heterogeneous catalysis is a key technology in industry because it enables the efficient synthesis of many base chemicals and fuels as well as their subsequent transformation into value-added products needed by our modern society [1]. Catalysis also plays an important role in several energy conversion technologies that will allow us to better utilize renewable energy sources [2,3]. To date, several of these sustainable energy applications still face significant challenges that limit their economic viability, partly due to the lack of suitable catalysts. The underlying principle of heterogeneous catalysis is that the interaction between the catalyst surface and the reactants reduces the activation barrier for the reaction, thereby accelerating the reaction. To improve on the performance of these catalysts, we generally look to alter their structural complexity through, e.g. nanostructuring, alloying, or by depositing the active component on suitable support materials, in order to derive a synergetic coupling between the reactions that can take place on the different materials [4–11]. An empirical search through different materials remains our primary approach towards catalyst discovery, but it is a time-consuming process. This approach also prevents the establishment of fundamental structure-property relationships that are needed to tailor the catalysts towards a structure where the activity, selectivity and stability are balanced in an optimal manner. Despite an increasingly sophisticated toolkit of synthesis methods at our disposal [12–16], it is still not possible to directly derive novel, low-cost, effective and long-term stable catalysts through rational design due to the lack of such knowledge [17–20].

Generating the understanding needed to rationally design optimized catalyst structures is not straightforward because it implies that we know the working structure of a catalyst and how this structure relates to the catalyst's activity, selectivity and stability [18,19]. The need to address the working structure of a catalyst under reaction or working conditions is far from trivial and has given rise to the development of what is commonly known as *in situ* and *operando* methods [21], where specialized reaction cells are added to conventional characterization instrumentation to enable studies of catalytic materials during reaction. Note that *operando* studies are a more narrowly defined subset of *in situ* studies where microscopy, spectroscopy or diffraction data of a sample collected under reaction conditions are coupled with simultaneous measurements of its catalytic performance (e.g. reaction rate measurements) to provide insights into the catalysts' activity and selectivity [22,23].

There has been rapid growth in the field of *in situ* and *operando* electron microscopy (EM) in recent years [24] due to the commercialization of environmental microscopes [25,26] and microfabricated environmental cells [27–30] that can be assembled within an electron microscope's sample stage/holder, Figure 1(a). In particular, modern *in situ* holders now include external connections to gas feed systems, fluid pumps, mass spectrometers, potentiostats and temperature control systems, unlocking the possibility of performing *operando* measurements. We emphasize here that for studies to be considered *operando*, the experiments must include direct measurement of the catalytic properties of the observed structures. This idea is exemplified in Figure 1(b)-(c) with results from Vendelbo *et al.*

[31] where oscillatory dynamics in Pt nanoparticles (NPs) are correlated with the fluctuations in gaseous product conversion measured with online mass spectrometry.

In this review, we will focus on how *in situ* and *operando* EM can be used to study chemical dynamics in catalysis over multiple length scales and to establish novel structure-property relationships. We aim to differentiate this review from other reviews on *in situ* EM by centering the discussion more on research in which EM is combined with measurements of the catalytic function or correlated with other techniques. The interested reader is referred to other existing reviews for a broader discussion of *in situ* EM [24,32–34]. We will also cover experimental setups for both, scanning electron microscopy (SEM) and transmission electron microscopy (TEM). In particular, we will highlight several examples of current research at the Fritz Haber Institute (FHI). *In situ* studies looking at the synthesis of NPs for catalytic applications [35,36] or the growth of nanostructures [37,38], including those mediated by metal catalysts will not be featured here. Besides a critical discussion on the importance of spatially-resolved *operando* experiments and their implementation, we also present examples of: (1) correlated studies where similar reaction cells are implemented across different instruments to combine *quasi in situ* or *in situ* EM observations with other techniques that provide a measure of the catalytic function or analysis of the chemical changes during reaction and (2) real-time studies where the performance is measured directly from the reaction cell within the EM chamber or column. In our opinion, both correlative and *operando* studies are needed to obtain a complete and comprehensive picture of the structural and chemical evolution of heterogeneous catalysts during reaction and the associated changes in activity and selectivity, which can span over several length scales.

## 1. On the importance of spatially-resolved operando experiments

Catalysts are metastable functional materials that constantly produce and consume active sites at the micro- and nanoscale under reaction conditions [39]. The fluctuating surface chemistry alters the surface reactivity, which in turn changes the catalyst activity and selectivity in the manner of a feedback loop. This dynamic consumption and formation of active phases underlie their chemical dynamics. The typical length and time scales of dynamical processes that can take place during catalytic reactions are illustrated in Figure 2(a) (from [19]). We highlight here that chemical dynamics can have different contributions and can involve both, reversible dynamics and irreversible transformations (that can cause deactivation) [40]. Chemical dynamics occur locally and can vary in both space and time. Their different contributions depend on the gradient of chemical potential along the interface between the catalyst and its entire environment [41].

The term “chemical potential” was first suggested by Bancroft, a PhD student of Ostwald, who was searching for an expression to clearly distinguish between electric potential and the intrinsic potential previously described by Gibbs [42]. The chemical potential μ of a component *i* reflects the partial molar

Gibbs free energy (1) of matter in a multi-component system with fixed parameters [42,43] and can be, for instance, expressed as follows:

$$\mu_i = \left(\frac{\partial G}{\partial n_i}\right)_{V,T,p,n_{j,\mathrm{pH};\, n_i \neq n_j}} \quad (1)$$

where G reflects the Gibbs free energy, $n_i$ and $n_j$ the number of components *i* and *j*, V and T represent the electric potential and temperature, respectively, and p denotes the pressure. Such a multi-component system can be, for instance, found in catalytic plug-flow reactors for gas phase reactions (Figure 2(b)) or the standardized electrocatalytic cells for liquid phase reactions. The value of *i* that has to be considered for different chemical potentials $\mu(V,T,p,pH,n_j)$ equals the number of elements present in the solid (e.g. phases or defects) and in the reaction environment (e.g. liquid or gas phase), including impurities [44].

In general, the surface can be considered equilibrated with the bulk after thermal pre-treatment and is then linked to its Gibbs free energy [45]. Although equilibrated in energy, the surface and bulk of a catalyst can differ in structure and composition [42]. It is common to find local compositional and structural gradients as we transit from the surface into the bulk, rendering a macroscopically homogeneous sample heterogeneous on the nanoscale [46]. Further changes in the surface free energy depend on the chemical potential gradient of the individual components in the reaction environment, which can be stimulated by external parameters such as electric potential or temperature, partial pressures or pH. Changes in these parameters induce a potential gradient between the reaction environment and the solid, leading to the solid adapting its surface states (e.g. morphology, composition, phase) until equilibrium is attained again. We explain this idea using the example of a gas phase reaction. The activation period of a catalyst, i.e. when the temperature, partial pressures or system pressure change, resembles a non-equilibrated system and the surface re-structures according to the chemical potential gradient to compensate for the potential differences. Hence, the catalyst tries to attain a new equilibrium morphology that can be metastable under the prescribed conditions, or in some cases, enter an oscillatory state where the catalyst alternates between two metastable structures [47,48]. We also highlight here that recent work using both SEM [49] and TEM [31] has demonstrated the possibility of visualizing such oscillatory dynamics.

Hence, the working structure of a catalyst can be very different from its as-prepared state (Figure 3(a)-(b)) [20,50]. It is worth mentioning that some surface states are only stable under working conditions [51,52] and can be localized at microscopic and atomic scales [53]. In addition, our understanding of such heterogeneities is complicated by the diverse synthesis and activation protocols used by different research groups, as well as variations in the structure/composition of the catalysts and local gradients in the chemical environment [46,54–56]. Here, we further differentiate between intrinsic

structural factors that are controlled by how the catalytic materials (or "pre-catalysts") are prepared and extrinsic reaction-induced factors that originate from the introduction of the reaction environment or heterogeneities in the reaction system (Figure 4).

Catalyst synthesis and pre-treatments methods dictate the intrinsic structure of a catalyst (Figure 4, left), which in turn influence distributions and concentrations of bulk and surface defects [46,56,57], dopants [58–60], surface strain [61], surface atomic enrichments [62], exposed lattice planes [63–65] and d-band shifts [66,67]. In the case of supported catalysts, we also need to consider metal-support interfaces [68–70], metal-support interactions [71–76], local curvature effects [77] and confinement effects within porous/hollow materials such as zeolites [78,79] and carbon nanotubes [80]. Small changes in any of these parameters can affect the overall catalytic performance. As a whole, the discrepancy between the complex structure of a real catalyst and the more commonly studied idealized model systems can be summed up as a "materials gap" [81–83].

Changes caused by the reaction environment (Figure 4, right) include surface reconstruction [84–87], surface segregation [88–90], selective oxidation of one component of the catalyst [91,92], metal dissolution [87,93–95], sintering [96–100], agglomeration [87], catalyst deactivation [41,87,96,101,102] and (frustrated) phase transitions [40,41]. In addition, the structural rearrangement can be a multiscale phenomenon [19,39]. The inhomogeneous environment of a catalytic reactor can lead to varying heats of reaction in different parts of the reactor [103] and non-uniform mass transport processes, which in turn creates temperature [104] and chemical potential [105–107] gradients. These gradients can affect the morphology of the catalytic particles over several length scales. There may also be variations in electron transfer between the surface and the bulk of a catalyst, which lead to band bending [108]. The difficulty in obtaining the complete description of a catalytic system can even be compounded by factors such as impurities in the gas feed [44,109]. Some of these myriad effects are pressure dependent and have led to the term of "pressure gap" [82,110–112] in gas phase studies to capture the differences between model catalysts studied using ultra-high vacuum characterization techniques versus that of catalysts under actual reaction conditions .

Here, we use the fixed bed of a standard plug-flow reactor to exemplify the impact of these inhomogeneities, Figure 2(b). Along the gas-flow direction, the fixed bed can be considered as infinitesimal slabs (Figure 2(c), inset: white rectangles). As the gas flows through different layers, an endo- or exothermic reaction can take place that changes the local gas composition in each slab, which in turn, alters the local catalytic structures and brings about a feedback cycle that affects the catalytic reactivity [107,113]. The analyzer, on the other hand, reports a catalytic conversion that is integrated over the different localized reaction conditions within the fixed-bed. An assumption of catalyst homogeneity forms the basis of most *ex situ* studies, where the before and after reaction structures of arbitrarily selected catalysts are compared. Such *ex situ* analysis may lead to controversial conclusions

because the catalyst morphologies can vary depending on which part of a bulk sample they are extracted from. Furthermore, the structures and oxidation states that form during reaction may be unstable and not detectable in samples analyzed outside the reaction environment (i.e. *ex situ*), which lead to an incorrect interpretation of the active structure or chemical species. Additional examples of such artifacts include drying or residual electrolyte artifacts for electrocatalysts that work in liquid environments, unstable oxides that are not present in the absence of the applied potential, and surface re-oxidation in the absence of a reducing reaction environment. Moreover, it is difficult to determine whether the catalysis-induced structural changes observed *ex situ* are beneficial or detrimental to the catalytic conversion. Decoupling the different effects that may be present is challenging without detailed insight into the structural evolution of these catalysts under working conditions.

While the structural pluralism between pristine and working catalytic structures was not included in Ostwald's definition of a catalytic process [114], he was aware that there is a "dependence of this [acceleration and retardation] of a chemical reaction on the nature and concentration of the catalysts, the temperature, the presence of other substances, etc.". A reliable comparison of catalytic results and mechanisms requires not only the investigation of structural and compositional identical materials and identical operation conditions [115] in gas (i.e. reactant gas composition/purity, pressure and temperature) and liquid (i.e. reactant concentrations, hydrodynamic conditions and applied potential) environments. In recent years, a plethora of different *operando* techniques have been developed for this purpose. Vibrational spectroscopy can be used to track adsorbed surface species such as spectator species (species that form at the surface but are not directly involved in the catalytic conversion), redox transitions, or changes in bond characteristics. X-ray diffraction can deliver phase information of the crystalline parts of the sample, whereas X-ray spectroscopy tracks the evolution of electronic surface states or changes in the interatomic distances and coordination number of bulk constituents [50,54,116–124]. Although these *operando* measurements have delivered valuable information and correlations on how the surface and bulk states evolve during the catalytic reaction, they still average over bulk and surface characteristics of the samples, thereby limiting the insight into the spatial distribution, spatial interactions between individual catalysts or catalyst components and the spatiotemporal evolution on the microscopic and nanoscopic scales.

Among these techniques, EM is unique as it is the only method that can probe the structure of catalysts on the micro- and nanoscale with very high spatial (nanometers down to atoms) and relatively high temporal resolution (typically in the order of milliseconds). In addition, the interaction of the electron beam with the sample generates spectroscopic signatures that can be used for complementary chemical analysis. This combination of high spatial resolution and spectroscopic capabilities make EMs ideal for studying the structure of nanoscale catalysts, especially those that consist of metal NPs [125–128]. For instance, TEM images are often the only way to establish local structures in these materials (examples in Figure 3), especially in the case of single-atom catalysts [129]. Therefore, EMs are

indispensable tools for catalyst characterization, even without considering their potential for *in situ* or *operando* studies.

## 2. Electron microscopy of heterogeneous catalysts

There is a long history in the materials science community related to using electrons to visualize the morphology and structure of materials. Unless mentioned explicitly, EM in this review refers to methods where electrons of several kilovolts interact directly with the sample, i.e. scanning electron microscopy (SEM) and transmission electron microscopy (TEM), and where these electron beams are used to probe and to form an image or diffraction pattern of the sample. We briefly mention two other electron-based imaging techniques, low energy electron microscopy (LEEM), which produces images with decelerated electrons and photoemission electron microscopy (PEEM) which utilizes the photoelectric effect. Both methods are surface sensitive and allow for imaging catalytic surface reactions on the mesoscale. PEEM is also sensitive to work function changes, which has been used to capture how local reaction kinetics vary with the orientation of the grains in polycrystalline materials [130,131].

In a SEM, the electron beam is focused to a spot and scanned over the sample surface. The image is then formed by collecting the electrons that come off the sample with different detectors in the microscope chamber. SEM is usually a surface imaging technique. The most common signal collected is that of secondary electrons emitted from regions close to the surface, which are used to form an image of the sample's surface topography. The emission of secondary electrons is also sensitive to work function changes of the surface, similar to PEEM. Concurrently, other signals from the sample can be collected, which include the information obtained from backscattered electrons (image and diffraction), transmitted electrons if the sample is thin enough, and characteristic X-rays.

In general, TEMs form images with electrons that have been transmitted through the sample. Hence, for useful imaging and spectroscopy conditions, the typical sample thicknesses are below a few hundred nanometers. The TEM can also be operated in two modes: the parallel beam illumination TEM mode and the focused probe scanning TEM (STEM) mode. The images in the TEM mode are composed of amplitude and/or phase contrast, whereas in STEM mode it is possible to obtain images with solely Z-contrast. By virtue of the short effective wavelengths of the accelerated electrons and the ability to form fine electron probes, EMs generally have spatial resolution in the nanometer range or below. In particular, aberration-corrected TEMs can attain sub-angstrom spatial resolution [132,133]. Readers are referred to the various textbooks available for details about these instruments [134,135].

## 3. *Enabling real-time SEM and TEM analysis for heterogeneous catalysis*

In general, EMs require the sample to be placed in a high vacuum environment. There are two common approaches for introducing a reactive environment into SEM chambers and TEM columns [24,136,137] and both concepts can be traced back to the early days of EM developments [138–140]. The first approach involves installing differentially pumped apertures into the electron gun column and adding more vacuum pumping capacity to enable operation at elevated pressures, typically at about tens of millibars. With differentially pumped EMs, the sample is usually heated or biased through additional attachments, such as a bulk resistive heater, a laser, or holders/stages with added electrical contacts. Although these environmental SEMs (ESEMs) and TEMs (ETEMs) are usually used to study gaseous reactions, it is also possible to image water droplets or thin water films that are condensed on a cooled stage or sample holder [141–144].

The second approach involves the use of closed or windowed cells that are sealed against the vacuum of the microscope to encapsulate the gas or liquid environment. In this case, the encapsulating material needs to be thin enough for electrons to pass through. Currently, the most widespread materials for these cells are silicon nitride membranes [27], followed by graphene [145]. Although there have been earlier implementations of closed cells using other materials [136,146,147], the highly scalable production of silicon nitride membrane window frames, also known as “chips”, using microfabrication technology has enabled the release of commercial systems and facilitated the field’s growth [24]. Figure 5 shows some of the capabilities we have at the FHI, which combine both, home-built and commercial solutions.

Before we delve into the details of the different approaches, we emphasize that the importance of *operando* TEM studies lies in resolving local morphological and structural changes in individual particles (Figure 2(c) inset: shape of the particles) and metastable phases that form during reaction at high spatial resolution and correlating them to the overall catalytic activity. This information allows us to understand how model structures evolve under working conditions and may provide insight for extrapolation to real catalyst systems. In general, either differentially pumped ETEMs or *in situ* TEM holders can be used to follow catalysts during gas phase reactions, whereas *in situ* holders are overwhelmingly employed in liquid phase studies. In terms of spatial resolution in a gas environment, both approaches allow for lattice resolution (or better) imaging, [28,148,149] but the ETEM is generally expected to deliver better resolution and sensitivity [148]. On the other hand, the *in situ* holders can be easily modified to include measurements of catalytic function with a flow cell design and/or with potentiometry. It is also more straightforward to incorporate closed cell systems into the setups of other *operando* techniques. Due to these reasons, we place more emphasis on the closed cell approach with individual sections dedicated to studies of catalysts in gases and liquids. ESEMs/ETEMs are dealt with more briefly below and the interested reader is referred to existing reviews such as Refs. [150–153] for a more complete treatment. The catalytic reactions that have been studied with these methods and referenced in this review are summarized in Table 1.

***Environmental SEM***

For SEM, it is quite common to find commercial ESEMs that allow for the introduction of gases at pressures of tens of millibars and home-built examples of closed-cell setups for the static encapsulation of samples in liquids or electrochemical studies. Despite the lack of widespread adoption of ESEM for *operando* studies of catalysts, the surface sensitivity of secondary electrons has intriguing potential for studying catalyzed reactions. Research from our institute has demonstrated the use of ESEM for following the growth of 2-dimensional materials, such as graphene [154–156] and boron nitride [157], and the changes in surface coverages of adsorbed gas molecules on metal foils [158] during reaction. In particular, we highlight a study [158] where the initiation and propagation of reaction fronts and the spillover of activated species were observed in real-time with this approach, Figure 8(a)-(b). Catalysis-induced work function changes of the surface [158] and phase transitions [49,159], including surface reconstructions, can also be investigated on a mesoscopic scale and compared to individual nanoparticle imaging in TEM and be correlated to the catalytic conversion. In addition, the larger chamber volume of the SEM offers several possibilities for adding complementary measurement capabilities and integrating correlative techniques, which can enable enhanced interpretative depth in terms of visual, spectroscopic or diffractometric information from the same sample. Hence, we have also been exploring different home-built designs for studying catalysts under reaction conditions.

One implementation is described in [159], where we incorporated a quartz tube reactor into the chamber of an ESEM with a modified vacuum system for studying catalytic gas-phase reactions (schematic in Figure 5(b)). The quartz tube reactor was machined with holes for the electron beam to pass through and for secondary electrons to escape from. The samples are heated with a laser. Catalytic conversion is measured online with a quadrupole mass spectrometer connected to the outlet of the tube that is mounted inside the SEM chamber. Oxophilic metal surfaces tend to oxidize immediately, making it challenging to investigate the reactions that take place on these metal surfaces. Using our setup [159], we were able to stabilize oxophilic, metallic Ni surfaces in the absence of hydrogen (see Figure 8(c)-(e)). The combination of mass spectrometry data and real time imaging allows us to extract valuable information on the structure-activity relationships of heterogeneous catalysts and disentangle the reversible and irreversible contributions to their chemical dynamics. It was found that reversible oxide-metal phase transitions act as an initiator for the catalytic production of synthesis gas from $CO_2$ and $CH_4$. In addition, surface transformations seem to influence the shape of the surface oxides. In the long-term, the surface transformations were found to shift the product stoichiometries from that indicative of a partial oxidation of methane ($CO:H_2 > 1$) towards dry reforming of methane ($CO:H_2 = 1$).

We also took advantage of the larger chamber size to adapt a design from our *operando* X-ray photoelectron spectroscopy synchrotron setup for correlated liquid-phase studies [160–162] (Figure 8(f))

and are exploring the use of a commercial closed cell system (Figure 5(c)) with integrated flow and regular reference/counter electrodes [163] for *operando* electrochemical studies.

***Environmental TEM***

ETEMs allow the direct injection of the gas into the TEM column and observations of catalysts under pressurized conditions around tens of millibars. Figure 6 shows examples of recent ETEM work capturing the structure of catalyst materials under different gas environments to illustrate the spatial resolution that we can attain in such studies. Two studies where the authors report the imaging of adsorbed molecules on a catalyst's surface are further highlighted in Figure 7.

While the lower pressure in the reaction chamber of an ETEM and the absence of the encapsulating membranes allows for higher contrast images of the catalyst surfaces, the large dead volume of the system relative to the amount of catalyst makes more complicated to detect conversion [164–166] and, thus, to perform *operando* studies. The experimental concerns in such studies also include sample-impurity interaction that stems from contaminants (e.g. hydrocarbons from the vacuum system) present within the column of the ETEM, sample holder, and gaskets (e.g. Viton O-rings), which can change the appearance of the sample surface. Furthermore, the reduced pressure leads to different chemical potentials (eq. 1) that in turn induce different surface structures. As discussed above, the different surface structures will present different reactivities and so, it can be challenging to obtain robust structure-activity correlations from ETEM studies in the absence of conversion detection.

So far, two approaches have been developed to mitigate this issue. The first one uses electron energy-loss spectroscopy [164,165] to measure the local gas composition, and the second one increases the amount of catalyst available using a packed pellet [166] to enable measurements of the products by mass spectrometry. There have also been efforts to model the thermal and gas flow patterns in the ETEM [167] to obtain better extrapolation of the reactor conditions to that of a plug-flow reactor. Although it is possible to integrate additional capabilities such as light sources [168], complementary vibrational/optical spectroscopy [169] and secondary ion mass spectrometry [170] into an ETEM, they require specialized modifications to the microscope column that are complicated to do in a typical laboratory setting.

***In situ TEM holders for gas- and liquid-phase studies***

*In situ* TEM holders with closed fluid cells are now quite common, with off-the-shelf units being offered by several manufacturers. In current implementations, a pair of chips is stacked together and sealed with o-rings [29] that are installed within the holder, allowing for imaging in gases at atmospheric pressures and in liquid environments. In addition, the "chips" can be patterned during

microfabrication to include MEMS-based heaters, electrodes and other capabilities. Hence, these *in situ* holders increasingly sophisticated with built-in channels for gas or liquid flow and electrical wiring for applying different stimuli, such as sample heating or biasing.

*Operando TEM for studying gas-phase reactions*

In terms of gas pressure, the closed cell setups can be operated at variable pressures between near ambient to atmospheric or higher pressures [28]. Current commercial *in situ* TEM holders for gas-phase studies are generally rated for 1 bar operating pressure and are equipped with gas lines that can be connected to a manifold and electrical connections for heating. The samples are usually heated with MEMS-based thin film heaters [28,171] and less commonly, with a laser [172]. The microfabricated heaters have advantages in terms of their ability to rapidly change temperature and a relatively low thermal footprint, which greatly reduces the time needed for thermal stabilization.

We can also measure the conversion of gaseous products from the catalysts deposited inside these cells by connecting the outlet stream from the reaction cells to a mass spectrometer for analysis of the gases, as demonstrated by Vendelbo *et al.* [31] (Figure 1(c)). Furthermore, nanocalorimetry measurements from the MEMS heaters can be used to follow the heat transfer during the reaction. The detection of reaction products is largely limited by two parameters, the quantity of products generated and the internal dead-volume of the setup (i.e. volume of the tubes connecting the reaction cell and the mass spectrometer). In general, a relatively small amount of catalyst is sufficient to generate changes in the gas composition and cause a response in the mass spectrometer [31,41,51]. The dead volume creates a delay between the onset of the reaction and the time where the products are detected, which must be calibrated prior to the experiment. To minimize the diffusive spread of gaseous species during their passage through the gas lines, the length of the tubes connecting the holder and the mass spectrometer should be as short as possible. We also need to be aware of possible sticking of certain gas molecules to the internal walls of such tubes and choose the appropriate tubing material.

To achieve performance improvements over existing manufacturer-designed setups for the detection of gaseous products, we have implemented our own home-built gas setup, Figure 5(a) [100]. The setup features operation pressures between 20 mbar and 1000 mbar and is able to precisely control gas flows to rates as low as 2 µl/min. The low flows ensure that the entire gas stream (without bypassing) can be forwarded into the analysis system without reaching the saturation pressure of the mass spectrometer. In addition, the analysis system is further characterized by a low base pressure ($<10^{-8}$ mbar), where the mass spectrometer is sensitive enough to detect small changes in conversion from the little amount of catalyst that is usually deposited on the MEMS chips.

The behavior we observe in these holders may roughly mimic a “single slab” in a plug-flow reactor (Figure 2(b)), but care has to be taken in correlating the results to the “real world”. There are significant differences in the reactor geometry between this “slab” and samples in an actual thermal

catalysis reactor, which can lead to deviations in the local chemical potential of the catalysts and their resultant chemical dynamics. First, the catalyst particles are only deposited on one side of the cell. Hence, for NPs deposited in these µm-thick reaction cells, most of the gas flows over the active layer, whereas in plug flow reactors, fixed beds are used that allow the entire gas phase to interact with the surface of the entire catalytic ensemble [31,41]. Second, NPs are typically supported directly on the electron-transparent silicon nitride surface, which is not a typical support material and may be compositionally inhomogeneous at the local scale [173,174]. Such differences can lead to variations in the local metal-support interactions. Also, unlike NP catalysts on conventional supports, these NPs are thermally decoupled from each other, which can limit heat transfer and lead to different onset temperatures (Figure 2(c), inset) [41]. Thus, the results from these *operando* experiments can only be considered as representative of a "local activity" of the catalytic ensemble. In principle, we should be able to correlate the observations from these closed cells to a defined position within the fixed-bed (Figure 2(c)**,** arrows) if the kinetics are comparable and establish the position of the observed structures and their function within the complex catalytic activity space of a bulk system. How to realize such direct extrapolation of the catalytic data measured from these closed cells to the catalytic data of real reactor systems, nevertheless, remains an open question.

*Operando TEM for studying liquid-phase reactions*

As described earlier, the closed cells used for liquid-phase TEM investigations can be patterned with thin film electrodes to enable electrochemical studies [27] (Figure 1(a)). These cells are, in general, fabricated in the form of a standard three-electrode setup where there is a working electrode, a reference electrode and a counter electrode. The electrolyte is usually introduced into the reaction cell from the outside through integrated microfluidic tubing [175]. The most common applications of electrochemical liquid cell TEM include studying the electro-deposition of metals [27,176] and the dynamics in battery materials [177–180]. Lattice resolution imaging has been reported for liquid cell studies, but it is unlikely that this resolution can be achieved for electrochemical studies because such imaging conditions entail high electron fluxes exceeding 1000 $e^-/(Å^2 \cdot s)$ and liquid films thinner than 100 nm [181]. Even without considering the implications of electron beam-induced effects at high fluxes, it is difficult to rationalize how these very thin liquid films can be considered representative of realistic electrochemical conditions. The same applies to *in situ* EM studies where imaging through a gas bubble is suggested in order to improve the imaging conditions. Therefore, we will need to work with liquid layers that are in the order of a few hundred nanometers or more, which limit the resolution to a few nanometers [181,182]. Nevertheless, liquid cell TEM is expected to play a major role in improving our understanding of the behavior of electrocatalysts under working conditions [183,184], because we can directly study the morphological evolution and stability of the catalysts under different electrochemical conditions (for example, see Ref. [87] and [95]).

However, there are a few technical hurdles that still need to be overcome for more versatile TEM studies of electrocatalysts. First, the design for the electrochemical cells needs to be optimized. There are limited options available from the manufacturers in terms of the materials that can be selected as three electrodes and the exact electrode geometry. For example, an integrated standard reference, such as Ag-AgCl, will be preferred as compared to the thin film pseudo-Pt electrodes mostly available for studying electrocatalytic processes. It is known that the thin film pseudo-reference electrodes, typically made of Pt, have limited stability and reproducibility. Offsets between these pseudo-reference electrodes and standard reference electrodes under the same solution conditions have been reported [185–187]. With regards to the working electrode support, a range of materials will also be beneficial for studying support effects [11]. Second, better approaches are needed to deposit the catalysts on the liquid cells. Currently, catalysts are commonly deposited directly on the working electrode through drop casting, but this process lacks control because it is challenging to deposit the catalysts only on the micrometer-sized electrode and to manage the loading density. Moreover, adhesion of the deposited electrocatalysts to the electrode is not guaranteed. If the electrocatalyst loading is too low or it does not adhere well, the contribution of the catalysts to the overall electrochemical signal will be too small and it will be difficult to differentiate the catalyst signal from the background signal from the electrode support itself. Third, due to the very small liquid volumes of these cells, bubble formation poses a constant challenge for gas-evolving reactions, where the nucleation of a gas bubble will drive out most of the electrolyte from the reaction cell, greatly altering the chemical environment. The limited electrolyte volumes can also lead to concentration gradients in the electrolyte and result in local changes in the pH, or mass-transport-limited behavior that is not seen in benchtop studies.

Another practical concern that is especially relevant to liquid-phase imaging is contamination of the fluid stream due to the use of chemically reactive electrolytes that might negatively interact with the different components of the *in situ* holders, i.e. chips, o-rings, holder materials and tubing. Control experiments should be performed to establish that the observed behavior is not an artifact of such contamination or cross-contamination from different electrolytes between the experiments. To avoid damaging the holders, tests involving the holder materials should also be carried out whenever corrosive electrolytes are used (see [188] for a description of such tests).

Lastly, the only methods for measuring reaction kinetics with electrochemical liquid cell TEM are potentiometry or amperometry, but these electrochemical measurements do not provide direct insight into the reaction products. Analysis of the reaction products in the outlet liquid stream is important for determining the selectivity in the case of multiple-product reactions such as the $CO_2$ electrochemical reduction reaction ($CO_2$RR) [11,189]. However, this is a non-trivial challenge with current electrochemical cell designs. There is only a small amount of catalyst on a patterned working electrode, which is much smaller than the heated area in a gas-phase setup, resulting in minute amounts of reaction products. This is an area where novel cell designs or developments should be explored.

## 4. *General challenges in in situ/operando EM studies of catalytic reactions*

Here, we discuss three general challenges in *operando* EM studies and the best practices to mitigate them.

### *Mitigating electron beam-induced effects*

First, the artifacts that can be introduced by the highly energetic electrons are the key concern for *in situ/operando* EM studies. We emphasize here that all the techniques that employ energetic probes (electrons, lasers, X-rays etc.) come with the likelihood of radiation-induced damage [190]. However, only with EM one can directly visualize these beam-induced effects at high spatial resolution and so, use different control experiments to identify such effects. In this sense, it should be standard practice to confirm that the observed phenomena are not artifacts of the electron beam irradiation or of the small volume of reactants encapsulated within the microfabricated cells.

The mechanisms behind these beam-induced effects also vary between gases and liquids. For gases, it has been reported that the electron beam can generate ionized species and radicals [191] that can be stabilized in the case of hydrocarbons by inductive and mesomeric effects, respectively [192]. For liquids, the primary effects are mainly driven by radiolytic products generated by the passage of electrons through the liquid [193,194]. In addition, the electron beam may shift the outcome of the electrochemical measurements [185,186]. It has been proposed that radiolytic product scavengers can be used to mitigate the effects of the electron beam [195] or that these effects can be exploited as a form of chemical perturbation if they can be rationalized through modeling of the radiation chemistry [192]. These strategies are, however, still at their early stages. The exact imaging conditions that minimize beam-induced effects also differ and depend on the materials and reaction media. For metallic NPs in gases, there is a growing consensus that the electron flux should be much lower than 200 $e^-/(Å^2 \cdot s)$ [31,92,196]. This threshold is going to be even lower for processes in liquids, where the electron beam can already induce growth of NPs at the moderate electron fluxes mentioned above [193,197].

Since electron illumination is unavoidable, it is good practice to use the lowest possible electron flux (or electron dose rate) and confirm the absence of obvious beam-induced effects using comparative control studies. Otherwise, it will be difficult to determine if the chemical dynamics observed at catalyst surfaces with atomic resolution are induced by the adsorption of reactants and changes of the local chemical potential or by electron beam damage. Showing only image sequences where the catalysts have the same morphology at different electron fluxes can be misleading if the electron flux used is not low enough. Nevertheless, a generally accepted workflow to address this issue, as well as consensus over control experiments needed to confirm largely artifact-free imaging conditions are still lacking. Here, we suggest the following standard protocol for reporting *in situ*/*operando* EM results: (i)

comparisons between areas that were illuminated by the electron beam during the experiment and those that had not been illuminated by the electron beam, (ii) beam-on and beam-off studies of the catalysts under reaction conditions, (iii) extended electron beam illumination studies under non-reactive conditions to ensure catalyst stability under a given electron flux, (iv) systematic studies to find threshold values that can be considered safe for each gas composition or liquid electrolyte, (v) the electron flux must be reported in $e^-/(Å^2 \cdot s)$ or equivalent units and should be calibrated (it is still common to find papers with the flux reported as the current on the TEM fluorescent screen), and (vi) for electrochemical liquid cell experiments, it is also recommended that the thickness of the liquid layer is determined and reported.

A side-effect of working at low electron fluxes to minimize beam-induced effects is that it decreases the signal-to-noise ratio in the images, which then negatively impacts the spatial resolution [182,198]. Thus, a compromise between the magnification, the acquisition rate of the images and the imaging electron flux is needed, which also depends on the radiation tolerance of the sample. Note that the spatial resolution scales with the electron fluence (or dose) to a power of -¼ [182]. It means that a large increase in electron fluence per image is needed to marginally improve the noise-limited resolution. Conversely, it also means that we can work within a reasonable range of low electron fluxes without a significant degradation of the imaging resolution. In addition, more sensitive state-of-the-art cameras, such as the direct electron detection cameras used in cryogenic TEMs to image biological structures can be utilized to improve the resolution [51].

***Statistical significance of operando TEM observations***

Second, the acquisition of statistically significant datasets is an inherent issue with high-resolution EM. High-resolution imaging also means that the images have a small field-of-view and so, there is usually only one or two particles per image. It cannot be assumed that catalytic structures are identical over the entire sample (see for example, Figure 3(c)-(e)) and so, datasets containing many particles need to be acquired [46]. Collecting such datasets can be tedious, especially if the particles also need to be tilted into the right orientations. *In situ/operando* studies add to this challenge because observations involving multiple particles showing the same behavior are needed to conclude that the results are representative. Currently, there is no consensus over the number of observations that need to be reported, and *in situ* studies that use only a few particles to extrapolate the general behavior of catalysts, while undesirable, are still common.

Ideally, the experiments should be repeated with different reaction cells, while tracking at least several particles in a few different areas of the sample to ensure reproducibility and statistical significance. However, datasets that contain multiple particles that are tracked over extended periods of time are also difficult to handle. Currently, a single *in situ* image sequence can already run into several thousand frames, which is impossible to analyze and interpret by hand. Hence, automated approaches

are necessary to make sense of such datasets. Advanced computer vision and analysis approaches for facilitating such analysis is an emerging field which will be addressed further in Section 7.

***Correlating a catalyst's structure with its properties***

Third, it is not straightforward to correlate these local observations with their function because in catalysis, the metrics for performance are usually obtained from ensemble-averaging methods. These measurements describe the global behavior of catalysts, while assuming that the catalysts are homogeneous, or that the reaction environment is homogeneous across the entire sample area, which may be invalid assumptions [130]. Hence, finding a robust way to bridge the few-particle observations from EM with information obtained from other techniques is crucial, but this aspect of the field is still generally under-developed. It is also not straightforward to derive important information about catalytic processes, such as the dynamics of these surface adsorbates (especially in liquid) from electron imaging or electron interaction-based spectroscopic methods in the TEM, despite studies reporting the imaging of CO [199] and $H_2O$ [200] molecules adsorbed on catalyst surfaces with ETEM (Figure 7). Hence, multi-modal approaches that complement TEM with methods that can better probe these surface processes, such as SEM, PEEM, infrared or Raman spectroscopy, is a current frontier in the field. Using identical reaction setups [201] to bridge the length-scales in a correlated manner can also help link the limited statistics in EM studies with ensemble-averaging measurements.

Next, we describe two more EM approaches that can be used to complement the *in situ* studies to mitigate some of the above described challenges.

***Quasi in situ approach***

In the *quasi in situ* method, the reactor side of the system is modified to allow for investigations involving samples on a TEM grid. Here, the secure transfer of the sample between the microreactor and the TEM is accomplished without exposure to ambient air through the loading of a grid onto a vacuum transfer holder within a glovebox filled with an inert atmosphere [202]. Due to the minute amount of catalyst particles that can be deposited on a TEM grid, a highly sensitive proton transfer reaction mass spectrometer should be connected to the microreactor in order to monitor the catalytic conversion during the reaction. State-of-the-art proton transfer reaction mass spectrometers can exhibit sensitivities below 10 parts per trillion (ppt). This approach decouples the catalytic reaction from the imaging and ensures the highest attainable resolution of the SEM or TEM, since the resolution is not diminished by imaging through a gas or a liquid [182,198]. It also offers the advantage of well-controlled reaction conditions that can be made closer to actual reaction conditions, which is particularly important for high-pressure reactions that exceed a few bars of pressure. In general, *quasi in situ* imaging excludes the artifacts due to the interaction of the electron-beam with the reaction environment and can indicate the presence of reaction-induced atomic-scale changes in beam-sensitive materials. However, it does not provide

continuous capture of the reaction-induced chemical dynamics or immediate insights into the formation of metastable states during the reaction.

Identical location imaging where the TEM grid is removed from the electrolyte at different points of the reaction and rinsed to remove electrolyte from the grid prior to loading into the TEM is also quite often used for studies of electrocatalysts [203–207]. However, there are pitfalls to this approach. The rinsing step may damage the fragile support film of the grid and lead to sample loss. It can also be complicated to use identical location imaging to study oxophilic samples, even if the transfer is performed in a glovebox, as rinsing with water may already be enough to alter the surface structures. Furthermore, it does not address the issue of drying artifacts that can occur during the vacuum transfer of these hydrated interfaces. Finally, it might not reflect the active state of the catalyst since the measurements are not conducted under an applied electrical potential.

***Correlated microscopy and spectroscopy***

In correlative studies, *in situ* platforms are deployed across different characterization instruments to provide complementary insights into the reaction medium-solid interaction. It is increasingly common to find a combination of TEM and synchrotron X-ray techniques, such as X-ray absorption spectroscopy [52,201,208–210], diffraction [210,211] and imaging [212], being used to follow gas phase reactions. There are also examples of TEM combined with optical spectroscopy [52,86,201,209,213]. For electrocatalytic studies, the usual way to derive catalytic function is through potentiometry or amperometry measurements [214]. Despite the relatively widespread examples of electrochemical setups for performing *operando* studies using synchrotron X-rays [189,215], infrared spectroscopy [189,216] and Raman spectroscopy [189,217], there are only few instances where these techniques are combined with identical location [206,207] *or in situ* EM [162,218] to study electrocatalysts. It should be feasible to do so since closed cells similar to those used in the TEM holders have already been implemented in a X-ray absorption spectroscopy setup to follow the insertion and removal dynamics in lithium-ion battery materials during cycling [219]. Correlated studies can provide the critical insight needed to bridge local and ensemble-averaging measurements. For example, Li *et al.* [208] showed that the combination of *operando* X-ray spectroscopy and TEM are needed to adequately characterize the changes in the size of Pt NP catalysts during ethylene hydrogenation.

We also mention here that most of these correlated studies do not use a common *in situ/operando* platform across the different techniques and the catalytic function is commonly inferred from measurements of the same samples obtained from separate bulk-scale reaction cells (except [201,209]). In some cases, the comparisons may also be made using different samples, such as nanoparticles versus bulk single crystals. In our opinion, such comparisons can be misleading because there may be a variation in the catalyst behavior due to the sample geometry, environment or reaction conditions, especially when techniques with different operating regimes (e.g. the working pressure or

electrolyte volume) are used. We expect the development of unified platforms that can translate across different techniques (such as [201,209]) to become more important because they simplify data interpretation by ensuring a consistent sample geometry and environment between the different techniques and mitigate possible discrepancies that arise from sample inhomogeneities.

## 5. *Research examples: Heterogeneous catalysts in gaseous environments*

So far, a few gas-phase thermal catalysis reactions have been studied by *operando* TEM (see Table 1) with the most common being CO oxidation. The adsorption and oxidation of CO molecules are often viewed as a prototypical probe reaction for heterogeneous catalysis because of its relative simplicity and the immediate role of CO in more complex reactions [220]. Hence, it is also a benchmark reaction for validating different experimental techniques. As highlighted earlier in Figure 1, work by Vendelbo *et al.* [31] showing that we can track the structural oscillations in Pt NPs during CO oxidation was an important demonstration of the potential of holder-based closed cells for *operando* studies. More significantly, fluctuations in gaseous products and heat released/absorbed during reaction can be matched to the structural variations. Since then, the standard catalysts for CO oxidation, Pt [41,51,86], Pd [51] and Rh [51], have been examined by different groups in terms of the correlation between their morphological and structural features and their catalytic activity. Figure 9 show images obtained from our research looking at (a)-(b) the morphological evolution of Pt NPs during repeated thermal cycling under reaction conditions and (c) comparing the behaviors of different noble metal NPs under the same reaction conditions.

Pt NPs can exhibit subtle re-structuring at relatively low temperatures [86] and structural oscillations at intermediate temperatures [31]. Reference [41] disentangled the different contributions of chemical dynamics that could be assigned to the different activity regimes. After the initiation of the reaction, where the partial pressures of reactants and products change significantly as the amount of produced $CO_2$ increases with increasing temperature, morphological transformations prevail. These morphological transformations lead to the stabilization of low index facets over temperature cycling. Subsequent cycling experiments revealed that this thermodynamic transformation leads to the loss of activity. At steady conversion, i.e. when the partial pressures remain constant, structural bulk changes can be observed in the electron diffraction pattern, which may be due to reactant diffusion into the bulk. These changes can be interpreted as a frustrated phase transition that maintains the catalytic activity.

In contrast, Pd NPs exhibit a different behavior during CO oxidation (Figure 9 (c), 1$^{st}$ row) , where the formation of low-index facets is not due to a thermodynamic stabilization [51]. The addition of CO into the gas stream at 200-300 °C drives the re-structuring of the Pd NPs into to a low-index facet dominated structure that is essentially inactive due to the lack of undercoordinated sites on the NP surface. The Pd NPs then change from the faceted structure to a rounded structure when they are heated

to 400°C (which is above their ignition temperature). This structural transition also corresponds to the production of $CO_2$. More importantly, the low-index facets re-form, and the NPs again became inactive when they are cooled below their ignition temperature, indicating reversible morphological and catalytic behavior. Under similar conditions, Pt NPs show subtle restructuring consistent with that described in Figure 9(b), whereas Rh NPs reduce from an oxide form to a metallic form. These transformations are not reversed with decreasing temperature. The difference between Pt and Pd NPs illustrates the impact catalyst re-structuring can have on their relative catalytic activity at low temperature, since Pt NPs retain their activity below the ignition temperature, but Pd NPs are inactive at the same temperatures. The observation of reversible morphological dynamics in Pd NPs clearly illustrates the importance of investigating the catalyst structure under reaction conditions.

Lastly, we will briefly mention *in situ* research that looks at other reactions or more complex NP catalyst structures. Bremmer *et al.* [221] studied Co NPs under Fischer-Tropsch synthesis conditions and visualized the formation of graphitic shells on the NPs due to the Boudouard reaction. More recently, Wang *et al.* [222] reported the reverse of this reaction, where graphite etching was initiated by exciting localized surface plasmons in Al NPs and the formation of CO was confirmed using mass spectrometry. In terms of more complex catalysts, Tan *et al.* [92] compared the morphological changes that occur in bimetallic Ni-Pt NPs synthesized in phase-segregated and random alloy geometries under reductive, oxidative and mixed-gas environments. These studies show that the initial design of the catalysts influences their pathway of morphological evolution. The phase-segregated NPs evolve into a core-shell structure with internal voids, whereas the random alloy NPs phase separated into NiO and Pt regions. Another recent paper identified reversible changes in the surface structure of bimetallic Ni-Au NPs during $CO_2$ hydrogenation [52]. These studies, however, cannot be considered *operando*, as the changes of such multi-component structures were not directly correlated with the catalytic conversion. We emphasize two key aspects that are required for such correlation. The first is a precise calibration of the mass spectrometer response. The second is decoupling the impact of the individual components in the alloy NPs from the measured online conversion data. Such investigations are likely to be non-trivial endeavors because they will entail systematic comparative studies where a series of tailored and well-controlled sample families are followed in order to establish observable trends in their behavior.

## 6. *Research examples: electrocatalysts in liquids*

Research looking at electrocatalysts using liquid cell TEM has mainly focused on the oxygen evolution reaction (OER) and oxygen reduction reaction (ORR) (see examples in Figure 10 and Table 1), and following the stability of NP catalysts under applied potential or during potential cycling. These studies encompassed monometallic [223], bimetallic [95,224,225], and oxide [187] NPs. Figure 10(a) depicts a STEM image sequence following octahedral Pt–Ni alloy catalysts supported on carbon during

electrochemical cycling [95], which illustrates the structural information that we can obtain from such dynamical studies and how they can provide insight into time-resolved pathways of catalyst/support re-structuring and degradation. We also highlight another study [223] tracking the behavior of Pt catalysts inside commercial inks that are used in polymer electrolyte membrane fuel cells and their evolution under extended cycling (Figure 10(b)).

Another liquid phase catalytic reaction where *in situ* TEM can provide meaningful insight is $CO_2$RR. The electrocatalytic reduction of $CO_2$ to hydrocarbon and alcohol products is a promising strategy for energy conversion and the generation of chemical feedstocks [226]. However, the reaction is also complex with multiple reaction pathways and reaction products [189,227,228]. Therefore, several challenges remain in designing an electrocatalyst that is optimized in terms of activity, selectivity and stability. So far, there have only been a few studies using identical location imaging [229] or *in situ* imaging [218,230] to capture the changes in these catalysts during reaction. In Ref. [218], Li *et al.* used liquid cell TEM to capture the dynamical aggregation of Cu nanoparticle ensembles into larger, disordered nanostructures with enhanced selectivity towards $C_{2+}$ products during the application of a reductive potential. In Ref. [230], we adopted a different approach in terms of starting materials in order to better understand how model electrocatalysts evolve during this reaction and were able to track the stability of shape-controlled $Cu_2O$ cubes under $CO_2$RR relevant conditions. We first directly synthesized shaped-controlled cubic $Cu_2O$ particles onto the working electrode via electrochemical deposition using a mixture of 5 mM $CuSO_4$ and 5 mM KCl [231] (Figure 11(a)). Next, we switched the electrolyte to $CO_2$-saturated $KHCO_3$ using fluid flow and applied a reductive potential at which $CO_2$RR can take place (Figure 11(b)). There were two key findings from this work. Regarding the synthesis, we showed that the formation of cubes was due to the addition of $Cl^-$ ions to the $CuSO_4$ solutions and that we can achieve shape-selection by alternating the applied potential within a narrow potential window in which the deposited non-cubic particles dissolve, but the cubic ones do not. The second finding relates to the time-resolved imaging of the morphological changes in the synthesized particles under $CO_2$RR reaction conditions. These *in situ* observations show that highly dynamic changes can occur on the working electrode surface within the first few minutes of applying a reductive potential, which impacts our understanding of the actual structures that exist under reaction conditions in laboratory scale electrochemical setups.

Using electrochemical liquid cell TEM to study the stability and degradation of catalytic structures will become more routine and we expect these insights to be useful for informing catalyst design. Nevertheless, the true promise of the technique still lies more in providing key knowledge for structure-property correlations with the higher resolution of TEM, which will require the development of new techniques that also enable simultaneous spectroscopic characterization of the chemical composition of the catalyst and surface species.

## *7. Summary and Future Perspectives*

This review describes state-of-the-art *in situ* and *operando* EM setups and various research examples highlighting their potential for investigating gas- and liquid-phase catalytic reactions, especially when there is concurrent detection of catalytic conversion and selectivity. While conversion detection is more straightforward for gas-phase reactions studied in dedicated TEM systems, the development of novel approaches and cell designs should soon also allow us to overcome the intrinsic limitations of the current electrocatalytic liquid phase set-ups. Although we did not discuss studies involving photocatalytic materials, we mention that there are already efforts aimed at integrating light sources inside the electron microscope [168] or the TEM holder [232], including a commercial version. For further progress in the field there is a crucial need to establish comparative studies for a better control and understanding of the effect of the electron beam, which is the biggest obstacle towards deriving meaningful insight from these experiments.

We also expect future improvements in electron microscopy instrumentation, such as cameras and detectors, to continue to drive the growth of this field, especially in terms of enabling the capture of faster dynamics or rapid tomography to follow the evolving 3-dimensional (3D) structure of catalysts under reactions conditions [233]. As TEM only delivers a 2-dimensional projection image of a 3D object, *operando* tomography would allow us to overcome the limitations concerning the missing 3D information. Another key area of future development will be having the possibility of tracking fast changes in the local composition and electronic structure of the materials, which is still difficult with the current spectroscopy methods that are associated with EM. This area will benefit from more sensitive spectrometers that allow for a rapid acquisition of spectra with sufficient signal-to-noise ratios.

In terms of future perspectives involving additional techniques, we consider multi-modal approaches as a promising area to be further explored, since it will enhance the interpretative depth of the *in situ* and *operando* measurements. In particular, multi-technique integration using an identical holder is needed for correlated studies of the same catalytic material over several length scales. Including both, local and integrating methods into a single platform will leverage on the capabilities of different techniques to obtain a comprehensive picture of the catalytic processes.

On the other hand, we should also keep in mind that the multi-modal studies will still only represent a small slice of the overall working state of a catalytic system. Improving reaction cell designs so that we can approach real reactor kinetics is expected to be another core area of development as it will allow the investigation of dynamic systems under more realistic conditions.

In addition to advances in instrumentation and techniques, we envision exciting opportunities for improving the computational approaches that can be used to process and analyze the *in situ* EM

datasets, especially with machine learning [234–236]. As mentioned earlier in Section 4, we need to work at low electron fluxes to minimize beam-induced artifacts in *in situ* studies, which translates to noisy, low contrast images. However, the approaches we commonly use to separate/segment the particle from the background are still unable to extract all the information encoded within these noisy images [173,236]. De-noising and segmentation algorithms that can retrieve high spatial resolution information from these image sequences will be highly advantageous for moving the field towards "minimum dose" *operando* EM studies. Similarly, improving the algorithms used for automated feature identification and classification across all the images in these large *in situ* datasets will be necessary for extracting useful insight from such experiments [237,238].

In conclusion, we have described in this review the potential of *operando* electron microscopy research, its challenges and the future prospects regarding its application as fundamental technique for the understanding of heterogeneous catalysis under realistic reaction conditions in greater detail. We expect that these efforts will result in the in-depth insight required for the rational design of the next generation of catalysts for a more efficient conversion and utilization of renewable energy.

**Acknowledgement**

This work was funded by the European Research Council (ERC-725915, OPERANDOCAT) and the Deutsche Forschungsgemeinschaft (DFG, German Research Foundation) – project no. 388390466 – TRR 247, subprojects A4 and B7, project no. 406944504 – SPP 2080, and Germany´s Excellence Strategy – EXC 2008 – 390540038 – UniSysCat.

S.W.C and B.R.C gratefully acknowledge the assistance of the electron microscopy group within the AC department for their help in getting the efforts of the ISC Department in liquid phase electron microscopy started. We also appreciate the technical support of Dr. Stephanie Kühl.

T.L. and R.S. acknowledge the excellent work of previous and current members of the electron microscopy group of the AC department at FHI. In particular, we are grateful for the pioneering work of Prof. Dangsheng Su, Dr. Zhu-Jun Wang, Dr. Jing Cao, and Dr. Marc Georg Willinger for installation and initialisation of the ESEM at the AC department at FHI for catalysis research. We further highlight the passionate work of Dr. Zhu-Jun Wang and Dr. Marc Georg Willinger for developing a laser heating stage for sample heating within the ESEM and Dr. Luis Ernesto Sandoval-Diaz for implementing the quartz tube reactor. In addition, Dr. Juan Velasco-Velez, Dr. Luis Ernesto Sandoval-Diaz, and M.Sc. Lorenz Frevel are acknowledged for adapting the synchrotron cells to the ESEMs which now allows correlative ESEM/XPS/XAS analysis. These joined team efforts have transformed a commercial FEI Quanta into a suitable device for the investigation of heterogeneous catalysts. Furthermore, Dr. Ramzi Farra and Dr. Marc Georg Willinger, are acknowledged for installing the initial in-situ feed and analysis

system for gas-phase TEM investigations. Dr. Milivoj Plodinec is thanked for his work on transforming this setup into an operando package. In addition, Dr. Travis Jones is acknowledged for discussions on the chemical potential. Furthermore, all engineers of the AC department and members of the FHI workshops are thanked for construction and building the setups.

## References


[1] Bravo-Suárez J J, Chaudhari R V. and Subramaniam B 2013 Design of heterogeneous catalysts for fuels and chemicals processing: An overview *ACS Symp. Ser.* **1132** 3–68

[2] Friend C M and Xu B 2017 Heterogeneous catalysis: A central science for a sustainable future *Acc. Chem. Res.* **50** 517–21

[3] Rodríguez-Padrón D, Puente-Santiago A R, Balu A M, Muñoz-Batista M J and Luque R 2019 Environmental Catalysis: Present and Future *ChemCatChem* **11** 18–38

[4] Singh A K and Xu Q 2013 Synergistic Catalysis over Bimetallic Alloy Nanoparticles *ChemCatChem* **5** 652–76

[5] Mistry H, Varela A S, Kühl S, Strasser P and Cuenya B R 2016 Nanostructured electrocatalysts with tunable activity and selectivity *Nat. Rev. Mater.* **1** 16009

[6] Zhang L, Zhao Z J and Gong J 2017 Nanostructured Materials for Heterogeneous Electrocatalytic CO2 Reduction and Related Reaction Mechanisms *Angew. Chemie - Int. Ed.* **56** 11326–53

[7] Kumar G, Nikolla E, Linic S, Medlin J W and Janik M J 2018 Multicomponent Catalysts: Limitations and Prospects *ACS Catal.* 3202–8

[8] Strasser P, Gliech M, Kuehl S and Moeller T 2018 Electrochemical processes on solid shaped nanoparticles with defined facets *Chem. Soc. Rev.*

[9] Kim C, Dionigi F, Beermann V, Wang X, Möller T and Strasser P 2019 Alloy Nanocatalysts for the Electrochemical Oxygen Reduction (ORR) and the Direct Electrochemical Carbon Dioxide Reduction Reaction (CO2RR) *Adv. Mater.* **31** 1–19

[10] Löffler T, Savan A, Garzón-Manjón A, Meischein M, Scheu C, Ludwig A and Schuhmann W 2019 Toward a Paradigm Shift in Electrocatalysis Using Complex Solid Solution Nanoparticles *ACS Energy Lett.* **4** 1206–14

[11] Gao D, Arán-Ais R M, Jeon H S and Roldan Cuenya B 2019 Rational catalyst and electrolyte design for CO2 electroreduction towards multicarbon products *Nat. Catal.* **2** 198–210

[12] Buck M R and Schaak R E 2013 Emerging strategies for the total synthesis of inorganic nanostructures *Angew. Chemie - Int. Ed.* **52** 6154–78

[13] Ruditskiy A, Peng H-C and Xia Y 2016 Shape-Controlled Metal Nanocrystals for Heterogeneous Catalysis *Annu. Rev. Chem. Biomol. Eng.* **7** 327–48

[14] Gilroy K D, Ruditskiy A, Peng H-C, Qin D and Xia Y 2016 Bimetallic Nanocrystals:

Syntheses, Properties, and Applications *Chem. Rev.* **116** 10414–10472

[15] Yan Y, Du J S, Gilroy K D, Yang D, Xia Y and Zhang H 2017 Intermetallic Nanocrystals: Syntheses and Catalytic Applications *Adv. Mater.* **29**

[16] Liu L and Corma A 2018 Metal catalysts for heterogeneous catalysis: from single atoms to nanoclusters and nanoparticles *Chem. Rev.* **118** 4981–5079

[17] Prieto G and Schüth F 2015 Bridging the gap between insightful simplicity and successful complexity: From fundamental studies on model systems to technical catalysts *J. Catal.* **328** 59–71

[18] Seh Z W, Kibsgaard J, Dickens C F, Chorkendorff I, Nørskov J K and Jaramillo T F 2017 Combining theory and experiment in electrocatalysis: Insights into materials design *Science.* **355**

[19] Kalz K F, Kraehnert R, Dvoyashkin M, Dittmeyer R, Gläser R, Krewer U, Reuter K and Grunwaldt J D 2017 Future Challenges in Heterogeneous Catalysis: Understanding Catalysts under Dynamic Reaction Conditions *ChemCatChem* **9** 17–29

[20] Sharapa D I, Doronkin D E, Studt F and Grunwaldt J 2019 Moving Frontiers in Transition Metal Catalysis : Synthesis , Characterization and Modeling *Adv. Mater.* **31** 1807381

[21] Weckhuysen B M 2003 Operando spectroscopy: Fundamental and technical aspects of spectroscopy of catalysts under working conditions *Phys. Chem. Chem. Phys.* **5** 1

[22] Banares M A 2005 Operando methodology: Combination of in situ spectroscopy and simultaneous activity measurements under catalytic reaction conditions *Catal. Today* **100** 71–7

[23] Guerrero-Perez M O and Banares M A 2006 From conventional in situ to operando studies in Raman spectroscopy *Catal. Today* **113** 48–57

[24] Liu X, He B, Zhang Y and Chen L 2020 In-situ Transmission Electron Microscope Techniques for Heterogeneous Catalysis *ChemCatChem* **12** 1853-72

[25] Boyes E D and Gai P L 1997 Environmental high resolution electron microscopy and applications to chemical science *Ultramicroscopy* **67** 219–32

[26] Sharma R and Weiss K 1998 Development of a TEM to study in situ structural and chemical changes at an atomic level during gas-solid interactions at elevated temperatures *Microsc. Res. Tech.* **42** 270–80

[27] Williamson M J, Tromp R M, Vereecken P M, Hull R and Ross F M 2003 Dynamic microscopy of nanoscale cluster growth at the solid-liquid interface. *Nat. Mater.* **2** 532–6

[28] Creemer J F, Helveg S, Hoveling G H, Ullmann S, Molenbroek A M, Sarro P M and Zandbergen H W 2008 Atomic-scale electron microscopy at ambient pressure *Ultramicroscopy* **108** 993–8

[29] Franks R, Morefield S, Wen J, Liao D, Alvarado J, Strano M and Marsh C 2008 A study of nanomaterial dispersion in solution by wet-cell transmission electron microscopy *J. Nanosci. Nanotechnol.* **8** 4404–7

[30] Ring E A and de Jonge N 2010 Microfluidic system for transmission electron microscopy. *Microsc. Microanal.* **16** 622–9

[31] Vendelbo S B, Elkjær C F, Falsig H, Puspitasari I, Dona P, Mele L, Morana B, Nelissen B J, Van Rijn R, Creemer J F, Kooyman P J and Helveg S 2014 Visualization of oscillatory behaviour of Pt nanoparticles catalysing CO oxidation *Nat. Mater.* **13** 884–90

[32] Crozier P A and Hansen T W 2015 In situ and operando transmission electron microscopy of catalytic materials *MRS Bull.* **40** 38–45

[33] Li J, Johnson G, Zhang S and Su D 2019 In Situ Transmission Electron Microscopy for Energy Applications *Joule* **3** 4–8

[34] Hwang S, Chen X, Zhou G and Su D 2019 In Situ Transmission Electron Microscopy on Energy-Related Catalysis *Adv. Energy Mater.* **10** 1902105

[35] Liao H-G, Niu K and Zheng H 2013 Observation of growth of metal nanoparticles *Chem. Commun.* **49** 11720–7

[36] Kim B H, Yang J, Lee D, Choi B K, Hyeon T and Park J 2018 Liquid-Phase Transmission Electron Microscopy for Studying Colloidal Inorganic Nanoparticles *Adv. Mater.* **30** 1703316

[37] Ross F M 2010 Controlling nanowire structures through real time growth studies *Reports Prog. Phys.* **73**

[38] Winterstein J and Sharma R 2016 Growth of One-Dimensional Nanomaterials in the ETEM BT - Controlled Atmosphere Transmission Electron Microscopy: Principles and Practice ed T W Hansen and J B Wagner (Basel, Switzerland: Springer International Publishing) pp 213–35

[39] Schlögl R 2015 Heterogeneous catalysis *Angew. Chemie - Int. Ed.* **54** 3465–520

[40] Schlögl R 2017 Catalysis 4.0 *ChemCatChem* **9** 533–41

[41] Plodinec M, Nerl H C, Girgsdies F, Schlögl R and Lunkenbein T 2020 Insights into Chemical Dynamics and Their Impact on the Reactivity of Pt Nanoparticles during CO Oxidation by Operando TEM *ACS Catal.* **10** 3183–93

[42] Baierlein R 2001 The elusive chemical potential *Am. J. Phys.* **69** 423–34

[43] Chen L-Q 2019 Chemical potential and Gibbs free energy *MRS Bull.* **44** 520–3

[44] Jones T E, Wyrwich R, Böcklein S, Carbonio E A, Greiner M T, Klyushin A Y, Moritz W, Locatelli A, Menteş T O, Niño M A, Knop-Gericke A, Schlögl R, Günther S, Wintterlin J and Piccinin S 2018 The Selective Species in Ethylene Epoxidation on Silver *ACS Catal.* **8** 3844–52

[45] Rogal J 2006 *Stability, composition and function of palladium surfaces in oxidizing environments: A first-principles statistical mechanics approach* (Freie Universität, Berlin)

[46] Masliuk L, Heggen M, Noack J, Girgsdies F, Trunschke A, Hermann K E, Willinger M G, Schlögl R and Lunkenbein T 2017 Structural Complexity in Heterogeneous Catalysis: Cataloging Local Nanostructures *J. Phys. Chem. C* **121** 24093–103

[47] Ertl G 1991 Oscillatory kinetics and spatio-temporal self-organization in reactions at solid surfaces *Science.* **254** 1750–5

[48] Imbihl R and Ertl G 1995 Oscillatory Kinetics in Heterogeneous Catalysis *Chem. Rev.* **95** 697–733

[49] Cao J, Rinaldi A, Plodinec M, Huang X, Willinger E, Hammud A, Hieke S, Beeg S, Gregoratti L, Colbea C, Schlögl R, Antonietti M, Greiner M and Willinger M 2020 In situ observation of oscillatory redox dynamics of copper *Nat. Commun.* **11** 3544

[50] Bergmann A and Roldan Cuenya B 2019 Operando Insights into Nanoparticle Transformations during Catalysis *ACS Catal.* **9** 10020–43

[51] Chee S W, Arce-Ramos J M, Li W, Genest A and Mirsaidov U 2020 Structural changes in noble metal nanoparticles during CO oxidation and their impact on catalyst activity *Nat. Commun.* **11** 2133

[52] Zhang X, Han S, Zhu B, Zhang G, Li X, Gao Y, Wu Z, Yang B, Liu Y, Baaziz W, Ersen O, Gu M, Miller J T and Liu W 2020 Reversible loss of core–shell structure for Ni–Au bimetallic nanoparticles during CO2 hydrogenation *Nat. Catal.* **3** 411–7

[53] Reuter K and Scheffler M 2003 First-Principles Atomistic Thermodynamics for Oxidation Catalysis: Surface Phase Diagrams and Catalytically Interesting Regions *Phys. Rev. Lett.* **90** 4

[54] Frenkel A I, Cason M W, Elsen A, Jung U, Small M W, Nuzzo R G, Vila F D, Rehr J J, Stach E A and Yang J C 2014 Critical review: Effects of complex interactions on structure and dynamics of supported metal catalysts *J. Vac. Sci. Technol. A Vacuum, Surfaces, Film.* **32** 020801

[55] Li X, Teschner D, Streibel V, Lunkenbein T, Masliuk L, Fu T, Wang Y, Jones T, Seitz F, Girgsdies F, Rosowski F, Schlögl R and Trunschke A 2019 How to control selectivity in alkane oxidation? *Chem. Sci.* **10** 2429–43

[56] Scott S L 2019 The Burden of Disproof *ACS Catal.* **9** 4706–8

[57] Taylor H S 1925 A theory of the catalytic surface *Proc. R. Soc. London. Ser. A, Contain. Pap. a Math. Phys. Character* **108** 105–11

[58] Rossetti I, Pernicone N and Forni L 2001 Promoters effect in Ru/C ammonia synthesis catalyst *Appl. Catal. A Gen.* **208** 271–8

[59] Schlögl R 2003 Catalytic synthesis of ammonia - A "never-ending story"? *Angew. Chemie - Int. Ed.* **42** 2004–8

[60] Johnson G R and Bell A T 2016 Effects of Lewis acidity of metal oxide promoters on the activity and selectivity of Co-based Fischer-Tropsch synthesis catalysts *J. Catal.* **338** 250–64

[61] Amakawa K, Sun L, Guo C, Hävecker M, Kube P, Wachs I E, Lwin S, Frenkel A I, Patlolla A, Hermann K, Schlögl R and Trunschke A 2013 How strain affects the reactivity of surface metal oxide catalysts *Angew. Chemie - Int. Ed.* **52** 13553–7

[62] Hävecker M, Wrabetz S, Kröhnert J, Csepei L I, Naumann D'Alnoncourt R, Kolen'Ko Y V., Girgsdies F, Schlögl R and Trunschke A 2012 Surface chemistry of phase-pure M1 MoVTeNb oxide during operation in selective oxidation of propane to acrylic acid *J. Catal.* **285** 48–60

[63] Tian N, Zhou Z Y and Sun S G 2008 Platinum metal catalysts of high-index surfaces: from single-crystal planes to electrochemically shape-controlled nanoparticles *J. Phys. Chem. C* **112** 19801–17

[64] Zhou Z Y, Huang Z Z, Chen D J, Wang Q, Tian N and Sun S G 2010 High-index faceted platinum nanocrystals supported on carbon black as highly efficient catalysts for ethanol electrooxidation *Angew. Chemie - Int. Ed.* **49** 411–4

[65] Melzer D, Xu P, Hartmann D, Zhu Y, Browning N D, Sanchez-Sanchez M and Lercher J A 2016 Atomic-Scale Determination of Active Facets on the MoVTeNb Oxide M1 Phase and Their Intrinsic Catalytic Activity for Ethane Oxidative Dehydrogenation *Angew. Chemie - Int. Ed.* **55** 8873–7

[66] Teschner D, Wild U, Schlögl R and Paál Z 2005 Surface state and composition of a disperse Pd catalyst after its exposure to ethylene *J. Phys. Chem. B* **109** 20516–21

[67] Ma Y, Li F, Ren X, Chen W, Li C, Tao P, Song C, Shang W, Huang R, Lv B, Zhu H, Deng T and Wu J 2018 Facets Matching of Platinum and Ferric Oxide in Highly Efficient Catalyst

Design for Low-Temperature CO Oxidation *ACS Appl. Mater. Interfaces* **10** 15322–7

[68] Fu Q, Li W X, Yao Y, Liu H, Su H Y, Ding M, Gu X K, Chen L, Wang Z, Zhang H, Wang B and Bao X 2010 Interface-confined ferrous centers for catalytic oxidation *Science.* **328** 1141–4

[69] Fu Q, Yang F and Bao X 2013 Interface-confined oxide nanostructures for catalytic oxidation reactions *Acc. Chem. Res.* **46** 1692–701

[70] Fu Q and Bao X 2017 Surface chemistry and catalysis confined under two-dimensional materials *Chem. Soc. Rev.* **46** 1842–74

[71] Tauster S J, Fung S C and Garten R L 1978 Strong Metal-Support Interactions. Group 8 Noble Metals Supported on TiO2 *J. Am. Chem. Soc.* **100** 170–5

[72] Tauster S J, Fung S C, Baker R T K and Horsley J A 1981 Strong interactions in supported-metal catalysts *Science.* **211** 1121–5

[73] Tauster S J 1987 Strong Metal-Support Interactions *Acc. Chem. Res.* **20** 389–94

[74] David Logan A, Braunschweig E J, Datye A K and Smith D J 1988 Direct Observation of the Surfaces of Small Metal Crystallites: Rhodium Supported on TiO2 *Langmuir* **4** 827–30

[75] Braunschweig E J, Logan A D, Datye A K and Smith D J 1989 Reversibility of strong metal-support interactions on Rh TiO2 *J. Catal.* **118** 227–37

[76] Zander S, Kunkes E L, Schuster M E, Schumann J, Weinberg G, Teschner D, Jacobsen N, Schlögl R and Behrens M 2013 The role of the oxide component in the development of copper composite catalysts for methanol synthesis *Angew. Chemie - Int. Ed.* **52** 6536–40

[77] Kühl S, Gocyla M, Heyen H, Selve S, Heggen M, Dunin-Borkowski R E and Strasser P 2019 Concave curvature facets benefit oxygen electroreduction catalysis on octahedral shaped PtNi nanocatalysts *J. Mater. Chem. A* **7** 1149–59

[78] Sastre G and Corma A 2009 The confinement effect in zeolites *J. Mol. Catal. A Chem.* **305** 3–7

[79] Boronat M and Corma A 2019 What Is Measured When Measuring Acidity in Zeolites with Probe Molecules? *ACS Catal.* **9** 1539–48

[80] Pan X and Bao X 2011 The effects of confinement inside carbon nanotubes on catalysis *Acc. Chem. Res.* **44** 553–62

[81] Campbell C T, Daube K A and White J M 1987 Cu/ZnO(0001̄) and ZnOx/Cu(111): Model catalysts for methanol synthesis *Surf. Sci.* **182** 458–76

[82] Imbihl R, Behm R J and Schlögl R 2007 Bridging the pressure and material gap in heterogeneous catalysis *Phys. Chem. Chem. Phys.* **9** 3459

[83] Kuld S, Thorhauge M, Falsig H, Elkjær C F, Helveg S, Chorkendorff I and Sehested J 2016 Quantifying the promotion of Cu catalysts by ZnO for methanol synthesis *Science.* **352** 969–74

[84] Somorjai G A 1994 Surface reconstruction and catalysis *Annu. Rev. Phys. Chem.* **45** 721–51

[85] Coulman D J, Wintterlin J, Behm R J and Ertl G 1990 Novel mechanism for the formation of chemisorption phases: The (2×1)O-Cu(110) added row reconstruction *Phys. Rev. Lett.* **64** 1761–4

[86] Avanesian T, Dai S, Kale M J, Graham G W, Pan X and Christopher P 2017 Quantitative and Atomic-Scale View of CO-Induced Pt Nanoparticle Surface Reconstruction at Saturation Coverage via DFT Calculations Coupled with in Situ TEM and IR *J. Am. Chem. Soc.* **139** 4551–8

[87] Popović S, Smiljanić M, Jovanovič P, Vavra J, Buonsanti R and Hodnik N 2020 Stability and Degradation Mechanisms of Copper-Based Catalysts for Electrochemical CO2 Reduction *Angew. Chemie - Int. Ed.* **59** 14736–46

[88] Zhan W, Wang J, Wang H, Zhang J, Liu X, Zhang P, Chi M, Guo Y, Guo Y, Lu G, Sun S, Dai S and Zhu H 2017 Crystal Structural Effect of AuCu Alloy Nanoparticles on Catalytic CO Oxidation *J. Am. Chem. Soc.* **139** 8846–54

[89] Zou L, Li J, Zakharov D, Saidi W A, Stach E A and Zhou G 2017 Atomically Visualizing Elemental Segregation-Induced Surface Alloying and Restructuring *J. Phys. Chem. Lett.* **8** 6035–40

[90] Greiner M T, Cao J, Jones T E, Beeg S, Skorupska K, Carbonio E A, Sezen H, Amati M, Gregoratti L, Willinger M G, Knop-Gericke A and Schlögl R 2018 Phase Coexistence of Multiple Copper Oxides on AgCu Catalysts during Ethylene Epoxidation *ACS Catal.* **8** 2286–95

[91] Yin J, Shan S, Yang L, Mott D, Malis O, Petkov V, Cai F, Shan Ng M, Luo J, Chen B H, Engelhard M and Zhong C J 2012 Gold-copper nanoparticles: Nanostructural evolution and bifunctional catalytic sites *Chem. Mater.* **24** 4662–74

[92] Tan S F, Chee S W, Baraissov Z, Jin H, Tan T L and Mirsaidov U 2019 Real-Time Imaging of Nanoscale Redox Reactions over Bimetallic Nanoparticles *Adv. Funct. Mater.* **29** 1903242

[93] Topalov A A, Katsounaros I, Auinger M, Cherevko S, Meier J C, Klemm S O and Mayrhofer K J J 2012 Dissolution of platinum: Limits for the deployment of electrochemical energy

conversion? *Angew. Chemie - Int. Ed.* **51** 12613–5

[94] Cherevko S 2018 Stability and dissolution of electrocatalysts: Building the bridge between model and "real world" systems *Curr. Opin. Electrochem.* **8** 118–25

[95] Beermann V, Holtz M E, Padgett E, De Araujo J F, Muller D A and Strasser P 2019 Real-time imaging of activation and degradation of carbon supported octahedral Pt-Ni alloy fuel cell catalysts at the nanoscale using: In situ electrochemical liquid cell STEM *Energy Environ. Sci.* **12** 2476–85

[96] Molenbroek A M, Helveg S, Topsøe H and Clausen B S 2009 Nano-particles in heterogeneous catalysis *Top. Catal.* **52** 1303–11

[97] Houk L R, Challa S R, Grayson B, Fanson P and Datye A K 2009 The definition of "critical radius" for a collection of nanoparticles undergoing Ostwald ripening *Langmuir* **25** 11225–7

[98] Simonsen S B, Chorkendorff I, Dahl S, Skoglundh M, Sehested J and Helveg S 2011 Ostwald ripening in a Pt/SiO2 model catalyst studied by in situ TEM *J. Catal.* **281** 147–55

[99] Karapinar D, Huan N T, Ranjbar Sahraie N, Li J, Wakerley D, Touati N, Zanna S, Taverna D, Galvão Tizei L H, Zitolo A, Jaouen F, Mougel V and Fontecave M 2019 Electroreduction of CO2 on Single-Site Copper-Nitrogen-Doped Carbon Material: Selective Formation of Ethanol and Reversible Restructuration of the Metal Sites *Angew. Chemie - Int. Ed.* **58** 15098–103

[100] Plodinec M, Nerl H C, Farra R, Willinger M G, Stotz E, Schlögl R and Lunkenbein T 2020 Versatile Homebuilt Gas Feed and Analysis System for Operando TEM of Catalysts at Work *Microsc. Microanal.* **26** 220–8

[101] Argyle M and Bartholomew C 2015 Heterogeneous Catalyst Deactivation and Regeneration: A Review *Catalysts* **5** 145–269

[102] Lunkenbein T, Girgsdies F, Kandemir T, Thomas N, Behrens M, Schlögl R and Frei E 2016 Bridging the Time Gap: A Copper/Zinc Oxide/Aluminum Oxide Catalyst for Methanol Synthesis Studied under Industrially Relevant Conditions and Time Scales *Angew. Chemie - Int. Ed.* **55** 12708–12

[103] Wismann S T, Engbæk J S, Vendelbo S B, Bendixen F B, Eriksen W L, Aasberg-Petersen K, Frandsen C, Chorkendorff I and Mortensen P M 2019 Electrified methane reforming: A compact approach to greener industrial hydrogen production *Science* **364** 756–9

[104] Jarenwattananon N N, Glöggler S, Otto T, Melkonian A, Morris W, Burt S R, Yaghi O M and Bouchard L S 2013 Thermal maps of gases in heterogeneous reactions *Nature* **502** 537–9

[105] Horn R, Korup O, Geske M, Zavyalova U, Oprea I and Schlögl R 2010 Reactor for in situ

measurements of spatially resolved kinetic data in heterogeneous catalysis *Rev. Sci. Instrum.* **81** 064102

[106] Korup O, Mavlyankariev S, Geske M, Goldsmith C F and Horn R 2011 Measurement and analysis of spatial reactor profiles in high temperature catalysis research *Chem. Eng. Process. Process Intensif.* **50** 998–1009

[107] Korup O, Goldsmith C F, Weinberg G, Geske M, Kandemir T, Schlögl R and Horn R 2013 Catalytic partial oxidation of methane on platinum investigated by spatial reactor profiles, spatially resolved spectroscopy, and microkinetic modeling *J. Catal.* **297** 1–16

[108] Heine C, Hävecker M, Sanchez-Sanchez M, Trunschke A, Schlögl R and Eichelbaum M 2013 Work function, band bending, and microwave conductivity studies on the selective alkane oxidation catalyst MoVTeNb oxide (orthorhombic M1 phase) under operation conditions *J. Phys. Chem. C* **117** 26988–97

[109] Wyrwich R, Jones T E, Günther S, Moritz W, Ehrensperger M, Böcklein S, Zeller P, Lünser A, Locatelli A, Menteş T O, Niño M Á, Knop-Gericke A, Schlögl R, Piccinin S and Wintterlin J 2018 LEED- i (V) Structure Analysis of the (7 × √3)rect SO4 Phase on Ag(111): Precursor to the Active Species of the Ag-Catalyzed Ethylene Epoxidation *J. Phys. Chem. C* **122** 26998–7004

[110] Over H and Muhler M 2003 Catalytic CO oxidation over ruthenium - Bridging the pressure gap *Prog. Surf. Sci.* **72** 3–17

[111] Reuter K, Frenkel D and Scheffler M 2004 The steady state of heterogeneous catalysis, studied by first-principles statistical mechanics *Phys. Rev. Lett.* **93** 116105

[112] Heine C, Hävecker M, Stotz E, Rosowski F, Knop-Gericke A, Trunschke A, Eichelbaum M and Schlögl R 2014 Ambient-pressure soft X-ray absorption spectroscopy of a catalyst surface in action: Closing the pressure gap in the selective n-butane oxidation over vanadyl pyrophosphate *J. Phys. Chem. C* **118** 20405–12

[113] Korup O, Schlögl R and Horn R 2012 Carbon formation in catalytic partial oxidation of methane on platinum: Model studies on a polycrystalline Pt foil *Catal. Today* **181** 177–83

[114] Ostwald W 1902 Catalysis *Nature* **65** 522–6

[115] Topsøe H 2003 Developments in operando studies and in situ characterization of heterogeneous catalysts *J. Catal.* **216** 155–64

[116] Li X, Wang H-Y, Yang H, Cai W, Liu S and Liu B 2018 In Situ/Operando Characterization Techniques to Probe the Electrochemical Reactions for Energy Conversion *Small Methods* **2**

1700395

[117] Arean C O, Weckhuysen B M and Zecchina a. 2012 Operando surface spectroscopy—placing catalytic solids at work under the spotlight *Phys. Chem. Chem. Phys.* **14** 2125

[118] Frenkel A I, Rodriguez J A and Chen J G 2012 Synchrotron techniques for in situ catalytic studies: Capabilities, challenges, and opportunities *ACS Catal.* **2** 2269–80

[119] Alayoglu S and Somorjai G A 2015 Nanocatalysis II: In Situ Surface Probes of Nano-Catalysts and Correlative Structure–Reactivity Studies *Catal. Letters* **145** 249–71

[120] Crumlin E J, Liu Z, Bluhm H, Yang W, Guo J and Hussain Z 2015 X-ray spectroscopy of energy materials under in situ/operando conditions *J. Electron Spectros. Relat. Phenomena* **200** 264–73

[121] Han H L, Melaet G, Alayoglu S and Somorjai G A 2015 In Situ Microscopy and Spectroscopy Applied to Surfaces at Work *ChemCatChem* **7** 3625–38

[122] Liu Y-S, Glans P-A, Arthur T S, Mizuno F, Chang C, Pong W-F and Guo J 2015 In-situ/operando soft x-ray spectroscopy characterization of interfacial phenomena in energy materials and devices *Sol. Hydrog. Nanotechnol. X* **9560** 956005

[123] Chakrabarti A, Ford M E, Gregory D, Hu R, Keturakis C J, Lwin S, Tang Y, Yang Z, Zhu M, Bañares M A and Wachs I E 2017 A decade+ of operando spectroscopy studies *Catal. Today* **283** 27–53

[124] Choi Y W, Mistry H and Roldan Cuenya B 2017 New insights into working nanostructured electrocatalysts through operando spectroscopy and microscopy *Curr. Opin. Electrochem.* **1** 95–103

[125] Su D S, Zhang B and Schlögl R 2015 Electron microscopy of solid catalysts - Transforming from a challenge to a toolbox *Chem. Rev.* **115** 2818–82

[126] Su D 2017 Advanced electron microscopy characterization of nanomaterials for catalysis *Green Energy Environ.* **2** 70–83

[127] Thomas J M 2017 Reflections on the value of electron microscopy in the study of heterogeneous catalysts *Proc. R. Soc. A Math. Phys. Eng. Sci.* **473**

[128] Zhang L, Shi W and Zhang B 2017 A review of electrocatalyst characterization by transmission electron microscopy *J. Energy Chem.* **26** 1117–35

[129] Chen Z W, Chen L X, Yang C C and Jiang Q 2019 Atomic (single, double, and triple atoms) catalysis: Frontiers, opportunities, and challenges *J. Mater. Chem. A* **7** 3492–515

[130] Suchorski Y, Spiel C, Vogel D, Drachsel W, Schlögl R and Rupprechter G 2010 Local Reaction Kinetics by Imaging: CO Oxidation on Polycrystalline Platinum *ChemPhysChem* **11** 3231–5

[131] Vogel D, Spiel C, Suchorski Y, Trinchero A, Schlögl R, Grönbeck H and Rupprechter G 2012 Local catalytic ignition during CO oxidation on low-index Pt and Pd surfaces: A combined PEEM, MS, and DFT study *Angew. Chemie - Int. Ed.* **51** 10041–4

[132] Girit Ç Ö, Meyer J C, Erni R, Rossell M D, Kisielowski C, Yang L, Park C-H, Crommie M F, Cohen M L, Louie S G and Zettl A 2009 Graphene at the Edge: Stability and Dynamics *Science.* **323** 1705 LP – 1708

[133] Krivanek O L, Chisholm M F, Nicolosi V, Pennycook T J, Corbin G J, Dellby N, Murfitt M F, Own C S, Szilagyi Z S, Oxley M P, Pantelides S T and Pennycook S J 2010 Atom-by-atom structural and chemical analysis by annular dark-field electron microscopy. *Nature* **464** 571–4

[134] Goldstein J I, Newbury D E, Michael J R, Ritchie N W M, Scott J H J and Joy D C 2017 *Scanning electron microscopy and x-ray microanalysis*

[135] Williams D B and Carter C B 2009 *Transmission Electron Microscopy: A Textbook for Materials Science* (New York, NY, NY: Springer Science+Business Media, LLC)

[136] Butler E P and Hale K F 1981 Dynamic experiments in the electron microscope *Practical Methods in Electron Microscopy volume 9* ed A M Glauert (Amsterdam, Netherlands: North-Holland) pp 239–355

[137] Tao F and Crozier P A 2016 Atomic-Scale Observations of Catalyst Structures under Reaction Conditions and during Catalysis *Chem. Rev.* **116** 3487–539

[138] Marton L 1934 Electron microscopy of biological objects *Phys. Rev.* **133** 527–8

[139] Ruska E 1942 Beitrag zur übermikroskopischen Abbildung bei höheren Drucken *Kolloid-Zeitschrift* **100** 212–9

[140] Abrams I M and Mcbain J W 1944 A closed cell for electron microscopy *Science.* **100** 273 LP – 274

[141] Donald A M 2003 The use of environmental scanning electron microscopy for imaging wet and insulating materials *Nat. Mater.* **2** 511–6

[142] Stokes D J 2003 Recent advances in electron imaging, image interpretation and applications: Environmental scanning electron microscopy *Philos. Trans. R. Soc. A Math. Phys. Eng. Sci.* **361** 2771–87

[143] Xiao J, Foray G and Masenelli-Varlot K 2018 Analysis of liquid suspensions using scanning electron microscopy in transmission: estimation of the water film thickness using Monte–Carlo simulations *J. Microsc.* **269** 151–60

[144] Levin B D A, Haiber D, Liu Q and Crozier P A 2019 An Open-Cell Environmental Transmission Electron Microscopy Technique for in Situ Characterization of Samples in Aqueous Liquid Solutions *Microsc. Microanal.* **26** 134–8

[145] Yuk J M, Park J, Ercius P, Kim K, Hellebusch D J, Crommie M F, Lee J Y, Zettl A and Alivisatos A P 2012 High-resolution EM of colloidal nanocrystal growth using graphene liquid cells. *Science.* **336** 61–4

[146] Parkinson G M 1989 High resolution, in-situ controlled atmosphere transmission electron microscopy (CATEM) of heterogeneous catalysts *Catal. Letters* **2** 303–7

[147] Giorgio S, Sao Joao S, Nitsche S, Chaudanson D, Sitja G and Henry C R 2006 Environmental electron microscopy (ETEM) for catalysts with a closed E-cell with carbon windows *Ultramicroscopy* **106** 503–7

[148] Helveg S, Kisielowski C F, Jinschek J R, Specht P, Yuan G and Frei H 2015 Observing gas-catalyst dynamics at atomic resolution and single-atom sensitivity *Micron* **68** 176–85

[149] Ek M, Jespersen S P F, Damsgaard C D and Helveg S 2016 On the role of the gas environment, electron-dose-rate, and sample on the image resolution in transmission electron microscopy *Adv. Struct. Chem. Imaging* **2** 4

[150] Hansen T W and Wagner J B 2014 Catalysts under controlled atmospheres in the transmission electron microscope *ACS Catal.* **4** 1673–85

[151] Jinschek J R 2014 Advances in the environmental transmission electron microscope (ETEM) for nanoscale in situ studies of gas-solid interactions *Chem. Commun.* **50** 2696-706

[152] Takeda S, Kuwauchi Y and Yoshida H 2015 Environmental transmission electron microscopy for catalyst materials using a spherical aberration corrector *Ultramicroscopy* **151** 178–90

[153] Hansen T W and Wagner J B 2016 *Controlled Atmosphere Transmission Electron Microscopy: Principles and Practice* (Basel, Switzerland: Springer International Publishing)

[154] Wang Z J, Weinberg G, Zhang Q, Lunkenbein T, Klein-Hoffmann A, Kurnatowska M, Plodinec M, Li Q, Chi L, Schloegl R and Willinger M G 2015 Direct observation of graphene growth and associated copper substrate dynamics by in situ scanning electron microscopy *ACS Nano* **9** 1506–19

[155] Wang Z J, Dong J, Cui Y, Eres G, Timpe O, Fu Q, Ding F, Schloegl R and Willinger M G

2016 Stacking sequence and interlayer coupling in few-layer graphene revealed by in situ imaging *Nat. Commun.* **7** 13256

[156] Wang Z J, Dong J, Li L, Dong G, Cui Y, Yang Y, Wei W, Blume R, Li Q, Wang L, Xu X, Liu K, Barroo C, Frenken J W M, Fu Q, Bao X, Schlögl R, Ding F and Willinger M G 2020 The Coalescence Behavior of Two-Dimensional Materials Revealed by Multiscale in Situ Imaging during Chemical Vapor Deposition Growth *ACS Nano* **14** 1902–18

[157] Wang L, Xu X, Zhang L, Qiao R, Wu M, Wang Z, Zhang S, Liang J, Zhang Z, Zhang Z, Chen W, Xie X, Zong J, Shan Y, Guo Y, Willinger M, Wu H, Li Q, Wang W, Gao P, Wu S, Zhang Y, Jiang Y, Yu D, Wang E, Bai X, Wang Z J, Ding F and Liu K 2019 Epitaxial growth of a 100-square-centimetre single-crystal hexagonal boron nitride monolayer on copper *Nature* **570** 91–5

[158] Barroo C, Wang Z-J, Schlögl R and Willinger M-G 2020 Imaging the dynamics of catalysed surface reactions by in situ scanning electron microscopy *Nat. Catal.* **3** 30–9

[159] Sandoval-Diaz L, Plodinec M, Ivanov D, Poitel S, Hammud A, Nerl H C, Schlögl R and Lunkenbein T 2020 Visualizing the importance of oxide-metal phase transitions in the production of synthesis gas over Ni catalysts *J. Energy Chem.* **50** 178–86

[160] Velasco-Vélez J J, Jones T E, Streibel V, Hävecker M, Chuang C H, Frevel L, Plodinec M, Centeno A, Zurutuza A, Wang R, Arrigo R, Mom R, Hofmann S, Schlögl R and Knop-Gericke A 2019 Electrochemically active Ir NPs on graphene for OER in acidic aqueous electrolyte investigated by in situ and ex situ spectroscopies *Surf. Sci.* **681** 1–8

[161] Velasco-Vélez J J, Jones T, Gao D, Carbonio E, Arrigo R, Hsu C J, Huang Y C, Dong C L, Chen J M, Lee J F, Strasser P, Roldan Cuenya B, Schlögl R, Knop-Gericke A and Chuang C H 2019 The Role of the Copper Oxidation State in the Electrocatalytic Reduction of CO 2 into Valuable Hydrocarbons *ACS Sustain. Chem. Eng.* **7** 1485–92

[162] Velasco-Velez J-J, Mom R V., Sandoval-Diaz L-E, Falling L J, Chuang C-H, Gao D, Jones T E, Zhu Q, Arrigo R, Roldan Cuenya B, Knop-Gericke A, Lunkenbein T and Schlögl R 2020 Revealing the Active Phase of Copper during the Electroreduction of CO 2 in Aqueous Electrolyte by Correlating In Situ X-ray Spectroscopy and In Situ Electron Microscopy *ACS Energy Lett.* **5** 2106–11

[163] Yoon A, Herzog A, Grosse P, Alsem D H and Chee S W 2020 Dynamic Imaging of Nanostructures in an Electrolyte with a Scanning Electron Microscope *Microsc. Microanal.* doi:10.1017/S1431927620024769

[164] Chenna S and Crozier P A 2012 Operando transmission electron microscopy: A technique for

detection of catalysis using electron energy-loss spectroscopy in the transmission electron microscope *ACS Catal.* **2** 2395–402

[165] Miller B K and Crozier P A 2014 Analysis of catalytic gas products using electron energy-loss spectroscopy and residual gas analysis for operando transmission electron microscopy *Microsc. Microanal.* **20** 815–24

[166] Miller B K, Barker T M and Crozier P A 2015 Novel sample preparation for operando TEM of catalysts *Ultramicroscopy* **156** 18–22

[167] Mortensen P M, Hansen T W, Wagner J B and Jensen A D 2015 Modeling of temperature profiles in an environmental transmission electron microscope using computational fluid dynamics *Ultramicroscopy* **152** 1–9

[168] Miller B K and Crozier P A 2013 System for in situ UV-visible illumination of environmental transmission electron microscopy samples *Microsc. Microanal.* **19** 461–9

[169] Picher M, Mazzucco S, Blankenship S and Sharma R 2015 Vibrational and optical spectroscopies integrated with environmental transmission electron microscopy *Ultramicroscopy* **150** 10–5

[170] Wirtz T, Philipp P, Audinot J N, Dowsett D and Eswara S 2015 High-resolution high-sensitivity elemental imaging by secondary ion mass spectrometry: From traditional 2D and 3D imaging to correlative microscopy *Nanotechnology* **26** 434001

[171] Allard L F, Overbury S H, Bigelow W C, Katz M B, Nackashi D P and Damiano J 2012 Novel MEMS-based gas-cell/heating specimen holder provides advanced imaging capabilities for in situ reaction studies *Microscopy and Microanalysis* **18** 656–66

[172] Mehraeen S, McKeown J T, Deshmukh P V., Evans J E, Abellan P, Xu P, Reed B W, Taheri M L, Fischione P E and Browning N D 2013 A (S)TEM gas cell holder with localized laser heating for in situ experiments *Microsc. Microanal.* **19** 470–8

[173] Chee S W, Anand U, Bisht G, Tan S F and Mirsaidov U 2019 Direct Observations of the Rotation and Translation of Anisotropic Nanoparticles Adsorbed at a Liquid-Solid Interface *Nano Lett.* **19** 2871–8

[174] Wang M, Dissanayake T U, Park C, Gaskell K and Woehl T J 2019 Nanoscale Mapping of Nonuniform Heterogeneous Nucleation Kinetics Mediated by Surface Chemistry *J. Am. Chem. Soc.* **141** 13516–24

[175] de Jonge N, Peckys D B, Kremers G J and Piston D W 2009 Electron microscopy of whole cells in liquid with nanometer resolution. *Proc. Natl. Acad. Sci. U. S. A.* **106** 2159–64

[176] Schneider N M, Park J H, Grogan J M, Steingart D A, Bau H H and Ross F M 2017 Nanoscale evolution of interface morphology during electrodeposition *Nat. Commun.* **8** 2174

[177] Gu M, Parent L R, Mehdi B L, Unocic R R, McDowell M T, Sacci R L, Xu W, Connell J G, Xu P, Abellan P, Chen X, Zhang Y, Perea D E, Evans J E, Lauhon L J, Zhang J-G G, Liu J, Browning N D, Cui Y, Arslan I and Wang C-M M 2013 Demonstration of an Electrochemical Liquid Cell for Operando Transmission Electron Microscopy Observation of the Lithiation/Delithiation Behavior of Si Nanowire *Nano Lett.* **13** 6106–12

[178] Unocic R R, Sun X G, Sacci R L, Adamczyk L A, Alsem D H, Dai S, Dudney N J and More K L 2014 Direct visualization of solid electrolyte interphase formation in lithium-ion batteries with in situ electrochemical transmission electron microscopy *Microsc. Microanal.* **20** 1029–37

[179] Layla Mehdi B, Gu M, Parent L R, Xu W, Nasybulin E N, Chen X, Unocic R R, Xu P, Welch D A, Abellan P, Zhang J-G, Liu J, Wang C-M, Arslan I, Evans J and Browning N D 2014 In-situ electrochemical transmission electron microscopy for battery research. *Microsc. Microanal.* **20** 484–92

[180] Holtz M E, Yu Y, Gunceler D, Gao J, Sundararaman R, Schwarz K A, Arias T A, Abruña H D and Muller D A 2014 Nanoscale imaging of lithium ion distribution during in situ operation of battery electrode and electrolyte. *Nano Lett.* **14** 1453–9

[181] de Jonge N and Ross F M 2011 Electron microscopy of specimens in liquid *Nat. Nanotechnol.* **6** 695–704

[182] de Jonge N, Houben L, Dunin-Borkowski R E and Ross F M 2019 Resolution and aberration correction in liquid cell transmission electron microscopy *Nat. Rev. Mater.* **4** 61–78

[183] Ross F M 2015 Opportunities and challenges in liquid cell electron microscopy *Science.* **350** aaa9886

[184] Hodnik N, Dehm G and Mayrhofer K J J 2016 Importance and Challenges of Electrochemical in Situ Liquid Cell Electron Microscopy for Energy Conversion Research *Acc. Chem. Res.* **49** 2015–22

[185] Schilling S, Janssen A, Zaluzec N J and Burke M G 2017 Practical Aspects of Electrochemical Corrosion Measurements during in Situ Analytical Transmission Electron Microscopy (TEM) of Austenitic Stainless Steel in Aqueous Media *Microsc. Microanal.* **23** 741–50

[186] Fahrenkrug E, Alsem D H, Salmon N and Maldonado S 2017 Electrochemical Measurements

in In Situ TEM Experiments *J. Electrochem. Soc.* **164** H358–64

[187] Ortiz Peña N, Ihiawakrim D, Han M, Lassalle-Kaiser B, Carenco S, Sanchez C, Laberty-Robert C, Portehault D and Ersen O 2019 Morphological and Structural Evolution of Co3O4 Nanoparticles Revealed by in Situ Electrochemical Transmission Electron Microscopy during Electrocatalytic Water Oxidation *ACS Nano* **13** 11372–81

[188] Chee S W and Burke M G 2016 Applications of Liquid Cell TEM in Corrosion Science *Liquid Cell Electron Microscopy* ed F M Ross (New York, NY: Cambridge University Press) pp 258–75

[189] Handoko A D, Wei F, Jenndy, Yeo B S and Seh Z W 2018 Understanding heterogeneous electrocatalytic carbon dioxide reduction through operando techniques *Nat. Catal.* **1** 922–34

[190] Henderson R 1995 The Potential and Limitations of Neutrons, Electrons and X-Rays for Atomic Resolution Microscopy of Unstained Biological Molecules *Q. Rev. Biophys.* **28** 171–93

[191] Koh A L, Gidcumb E, Zhou O and Sinclair R 2013 Observations of carbon nanotube oxidation in an aberration-corrected environmental transmission electron microscope *ACS Nano* **7** 2566–72

[192] Rehn S M and Jones M R 2018 New Strategies for Probing Energy Systems with in Situ Liquid-Phase Transmission Electron Microscopy *ACS Energy Lett.* **3** 1269–78

[193] Woehl T J, Jungjohann K L, Evans J E, Arslan I, Ristenpart W D and Browning N D 2013 Experimental procedures to mitigate electron beam induced artifacts during in situ fluid imaging of nanomaterials. *Ultramicroscopy* **127** 53–63

[194] Schneider N M, Norton M M, Mendel B J, Grogan J M, Ross F M and Bau H H 2014 Electron–Water Interactions and Implications for Liquid Cell Electron Microscopy *J. Phys. Chem. C* **118** 22373–82

[195] Woehl T J and Abellan P 2017 Defining the radiation chemistry during liquid cell electron microscopy to enable visualization of nanomaterial growth and degradation dynamics *J. Microsc.* **265** 135–47

[196] Ek M, Ramasse Q M, Arnarson L, Georg Moses P and Helveg S 2017 Visualizing atomic-scale redox dynamics in vanadium oxide-based catalysts *Nat. Commun.* **8** 305

[197] Woehl T J, Evans J E, Arslan I, Ristenpart W D and Browning N D 2012 Direct in situ determination of the mechanisms controlling nanoparticle nucleation and growth. *ACS Nano* **6** 8599–610

[198] Taheri M L, Stach E A, Arslan I, Crozier P A, Kabius B C, LaGrange T, Minor A M, Takeda S, Tanase M, Wagner J B and Sharma R 2016 Current status and future directions for in situ transmission electron microscopy *Ultramicroscopy* **170** 86–95

[199] Yoshida H, Kuwauchi Y, Jinschek J R, Sun K, Tanaka S, Kohyama M, Shimada S, Haruta M and Takeda S 2012 Visualizing gas molecules interacting with supported nanoparticulate catalysts at reaction conditions *Science.* **335** 317–9

[200] Yuan W, Zhu B, Li X Y, Hansen T W, Ou Y, Fang K, Yang H, Zhang Z, Wagner J B, Gao Y and Wang Y 2020 Visualizing H2O molecules reacting at TiO2 active sites with transmission electron microscopy *Science.* **367** 428–30

[201] Zhao S, Li Y, Stavitski E, Tappero R, Crowley S, Castaldi M J, Zakharov D N, Nuzzo R G, Frenkel A I and Stach E A 2015 Operando Characterization of Catalysts through use of a Portable Microreactor *ChemCatChem* **7** 3683–91

[202] Masliuk L, Swoboda M, Algara-Siller G, Schlögl R and Lunkenbein T 2018 A quasi in situ TEM grid reactor for decoupling catalytic gas phase reactions and analysis *Ultramicroscopy* **195** 121–8

[203] Mayrhofer K J J, Meier J C, Ashton S J, Wiberg G K H, Kraus F, Hanzlik M and Arenz M 2008 Fuel cell catalyst degradation on the nanoscale *Electrochem. commun.* **10** 1144–7

[204] Arán-Ais R M, Yu Y, Hovden R, Solla-Gullón J, Herrero E, Feliu J M and Abruña H D 2015 Identical Location Transmission Electron Microscopy Imaging of Site-Selective Pt Nanocatalysts: Electrochemical Activation and Surface Disordering *J. Am. Chem. Soc.* **137** 14992–8

[205] Arenz M and Zana A 2016 Fuel cell catalyst degradation: Identical location electron microscopy and related methods *Nano Energy* **29** 299–313

[206] Fan K, Zou H, Lu Y, Chen H, Li F, Liu J, Sun L, Tong L, Toney M F, Sui M and Yu J 2018 Direct Observation of Structural Evolution of Metal Chalcogenide in Electrocatalytic Water Oxidation *ACS Nano* **12** 12369–79

[207] Zhu Y, Chen H C, Hsu C S, Lin T S, Chang C J, Chang S C, Tsai L D and Chen H M 2019 Operando unraveling of the structural and chemical stability of P-substituted CoSe2 electrocatalysts toward hydrogen and oxygen evolution reactions in alkaline electrolyte *ACS Energy Lett.* **4** 987–94

[208] Li Y, Zakharov D, Zhao S, Tappero R, Jung U, Elsen A, Baumann P, Nuzzo R G, Stach E A and Frenkel A I 2015 Complex structural dynamics of nanocatalysts revealed in Operando

conditions by correlated imaging and spectroscopy probes *Nat. Commun.* **6** 7583

[209] Zhao S, Li Y, Liu D, Liu J, Liu Y M, Zakharov D N, Wu Q, Orlov A, Gewirth A A, Stach E A, Nuzzo R G and Frenkel A I 2017 Multimodal Study of the Speciations and Activities of Supported Pd Catalysts During the Hydrogenation of Ethylene *J. Phys. Chem. C* **121** 18962–72

[210] Tsoukalou A, Abdala P M, Stoian D, Huang X, Willinger M G, Fedorov A and Müller C R 2019 Structural Evolution and Dynamics of an In2O3 Catalyst for CO2 Hydrogenation to Methanol: An Operando XAS-XRD and in Situ TEM Study *J. Am. Chem. Soc.* **141** 13497–505

[211] Roobol S B, Onderwaater W G, Van Spronsen M A, Carla F, Balmes O, Navarro V, Vendelbo S, Kooyman P J, Elkjær C F, Helveg S, Felici R, Frenken J W M and Groot I M N 2017 In situ studies of NO reduction by H2 over Pt using surface X-ray diffraction and transmission electron microscopy *Phys. Chem. Chem. Phys.* **19** 8485–95

[212] Wu Y A, McNulty I, Liu C, Lau K C, Liu Q, Paulikas A P, Sun C J, Cai Z, Guest J R, Ren Y, Stamenkovic V, Curtiss L A, Liu Y and Rajh T 2019 Facet-dependent active sites of a single Cu2O particle photocatalyst for CO2 reduction to methanol *Nat. Energy* **4** 957–68

[213] Resasco J, Dai S, Graham G, Pan X and Christopher P 2018 Combining In-Situ Transmission Electron Microscopy and Infrared Spectroscopy for Understanding Dynamic and Atomic-Scale Features of Supported Metal Catalysts *J. Phys. Chem. C* **122** 25143–57

[214] Sebastián-Pascual P and Escudero-Escribano M 2020 Addressing the Interfacial Properties for CO Electroreduction on Cu with Cyclic Voltammetry *ACS Energy Lett.* **5** 130–5

[215] Nagasaka M, Yuzawa H and Kosugi N 2015 Development and application of in situ/operando soft X-ray transmission cells to aqueous solutions and catalytic and electrochemical reactions *J. Electron Spectros. Relat. Phenomena* **200** 293–310

[216] Zaera F 2014 New advances in the use of infrared absorption spectroscopy for the characterization of heterogeneous catalytic reactions *Chem. Soc. Rev.* **43** 7624–63

[217] Deng Y and Yeo B S 2017 Characterization of Electrocatalytic Water Splitting and CO2 Reduction Reactions Using in Situ/Operando Raman Spectroscopy *ACS Catal.* **7** 7873–89

[218] Li Y, Kim D, Louisia S, Xie C, Kong Q, Yu S, Lin T, Aloni S, Fakra S C and Yang P 2020 Electrochemically scrambled nanocrystals are catalytically active for CO2-to-multicarbons *Proc. Natl. Acad. Sci. U. S. A.* **117** 9194–201

[219] Lim J, Li Y, Alsem D H, So H, Lee S C, Bai P, Cogswell D A, Liu X, Jin N, Yu Y S, Salmon N J, Shapiro D A, Bazant M Z, Tyliszczak T and Chueh W C 2016 Origin and hysteresis of

lithium compositional spatiodynamics within battery primary particles *Science*. **353** 566–71

[220] Freund H J, Meijer G, Scheffler M, Schlögl R and Wolf M 2011 CO oxidation as a prototypical reaction for heterogeneous processes *Angew. Chemie - Int. Ed.* **50** 10064–94

[221] Bremmer G M, Zacharaki E, Sjåstad A O, Navarro V, Frenken J W M and Kooyman P J 2017 In situ TEM observation of the Boudouard reaction: Multi-layered graphene formation from CO on cobalt nanoparticles at atmospheric pressure *Faraday Discuss.* **197** 337–51

[222] Wang C, Yang W C D, Raciti D, Bruma A, Marx R, Agrawal A and Sharma R 2020 Endothermic reaction at room temperature enabled by deep-ultraviolet plasmons *Nat. Mater.* doi:10.1038/s41563-020-00851-x

[223] Impagnatiello A, Cerqueira C F, Coulon P E, Morin A, Escribano S, Guetaz L, Clochard M C and Rizza G 2020 Degradation Mechanisms of Supported Pt Nanocatalysts in Proton Exchange Membrane Fuel Cells: An Operando Study through Liquid Cell Transmission Electron Microscopy *ACS Appl. Energy Mater.* **3** 2360–71

[224] Zhu G Z, Prabhudev S, Yang J, Gabardo C M, Botton G A and Soleymani L 2014 In situ liquid cell TEM study of morphological evolution and degradation of Pt-Fe nanocatalysts during potential cycling *J. Phys. Chem. C* **118** 22111–9

[225] Tan S F, Chee S W, Baraissov Z, Jin H, Tan T L and Mirsaidov U 2019 Intermediate Structures of Pt-Ni Nanoparticles during Selective Chemical and Electrochemical Etching *J. Phys. Chem. Lett.* **10** 6090–6

[226] De Luna P, Hahn C, Higgins D, Jaffer S A, Jaramillo T F and Sargent E H 2019 What would it take for renewably powered electrosynthesis to displace petrochemical processes? *Science.* **364** 6438

[227] Nitopi S, Bertheussen E, Scott S B, Liu X, Engstfeld A K, Horch S, Seger B, Stephens I E L, Chan K, Hahn C, Nørskov J K, Jaramillo T F and Chorkendorff I 2019 Progress and Perspectives of Electrochemical CO2 Reduction on Copper in Aqueous Electrolyte *Chem. Rev.* **119** 7610–72

[228] Birdja Y Y, Pérez-Gallent E, Figueiredo M C, Göttle A J, Calle-Vallejo F and Koper M T M 2019 Advances and challenges in understanding the electrocatalytic conversion of carbon dioxide to fuels *Nat. Energy* **4** 732–45

[229] Osowiecki W T, Nussbaum J J, Kamat G A, Katsoukis G, Ledendecker M, Frei H, Bell A T and Alivisatos A P 2019 Factors and Dynamics of Cu Nanocrystal Reconstruction under CO2 Reduction *ACS Appl. Energy Mater.* **2** 7744–9

[230] Arán-Ais R M, Rizo R, Grosse P, Algara-Siller G, Dembélé K, Plodinec M, Lunkenbein T, Chee S W and Cuenya B R 2020 Imaging electrochemically synthesized Cu2O cubes and their morphological evolution under conditions relevant to CO2 electroreduction *Nat. Commun.* **11** 3489

[231] Grosse P, Gao D, Scholten F, Sinev I, Mistry H and Roldan Cuenya B 2018 Dynamic Changes in the Structure, Chemical State and Catalytic Selectivity of Cu Nanocubes during CO2 Electroreduction: Size and Support Effects *Angew. Chemie - Int. Ed.* **57** 6192–7

[232] Cavalca F, Laursen A B, Kardynal B E, Dunin-Borkowski R E, Dahl S, Wagner J B and Hansen T W 2012 In situ transmission electron microscopy of light-induced photocatalytic reactions *Nanotechnology* **23** 075705

[233] Roiban L, Li S, Aouine M, Tuel A, Farrusseng D and Epicier T 2018 Fast 'Operando' electron nanotomography *J. Microsc.* **269** 117–26

[234] Aguiar J A, Gong M L, Unocic R R, Tasdizen T and Miller B D 2019 Decoding crystallography from high-resolution electron imaging and diffraction datasets with deep learning *Sci. Adv.* **5** eaaw1949

[235] Yao L, Ou Z, Luo B, Xu C and Chen Q 2020 Machine Learning to Reveal Nanoparticle Dynamics from Liquid-Phase TEM Videos *ACS Cent. Sci.* **6** 1421–30

[236] Horwath J P, Zakharov D N, Mégret R and Stach E A 2020 Understanding important features of deep learning models for segmentation of high-resolution transmission electron microscopy images *npj Comput. Mater.* **6** 108

[237] Belianinov A, He Q, Kravchenko M, Jesse S, Borisevich A and Kalinin S V. 2015 Identification of phases, symmetries and defects through local crystallography *Nat. Commun.* **6** 7801

[238] Hussaini Z, Lin P A, Natarajan B, Zhu W and Sharma R 2018 Determination of atomic positions from time resolved high resolution transmission electron microscopy images *Ultramicroscopy* **186** 139–45

[239] Aouine M, Epicier T and Millet J M M 2016 In Situ Environmental STEM Study of the MoVTe Oxide M1 Phase Catalysts for Ethane Oxidative Dehydrogenation *ACS Catal.* **6** 4775–81

[240] He Y, Liu J C, Luo L, Wang Y G, Zhu J, Du Y, Li J, Mao S X and Wang C 2018 Size-dependent dynamic structures of supported gold nanoparticles in CO oxidation reaction condition *Proc. Natl. Acad. Sci. U. S. A.* **115** 7700–5

*Table 1. Summary of the reactions and methods referenced in this paper*

| Gas Phase Catalytic Reactions | | | |
|---|---|---|---|
| Reaction | Method | Paired with | References |
| Carbon Monoxide Oxidation | ETEM | | [33,166,199] |
| | Closed Cell | Online Mass Spectrometry | [31,41,51,92,100] |
| | Closed Cell | IR Spectroscopy | [86,213] |
| Carbon Dioxide Hydrogenation | ETEM | | [81] |
| | Closed Cell | Synchrotron X-ray Spectroscopy | [212] |
| | Closed Cell | Synchrotron X-ray and IR Spectroscopy | [52] |
| Ethane Dehydrogenation | ETEM | | [239] |
| Ethylene Hydrogenation | Closed Cell | Mass spectrometry, Synchrotron X-ray, IR and Raman Spectroscopy | [201,208,209] |
| Fischer-Tropsch | ESEM | Online Mass Spectrometry | [159] |
| Fischer-Tropsch | Closed Cell | Online Mass Spectrometry | [221] |
| Nitrogen Monoxide Reduction | Closed Cell | Synchrotron X-ray Diffraction | [211] |
| Reverse Boudouard | Closed Cell ETEM | Online Mass Spectrometry | [222] |
| Water Gas Shift | ETEM | | [200] |
| | | | |
| Liquid Phase Catalystic Reactions | | | |
| Carbon Dioxide Reduction | Closed Cell | | [230] |
| | Closed Cell | Synchrotron X-ray Spectroscopy | [162,218] |
| Oxygen Evolution | Closed Cell | Synchrotron X-ray, Raman Spectroscopy | [187] |
| Oxygen Reduction | Closed Cell | | [95,223,224] |

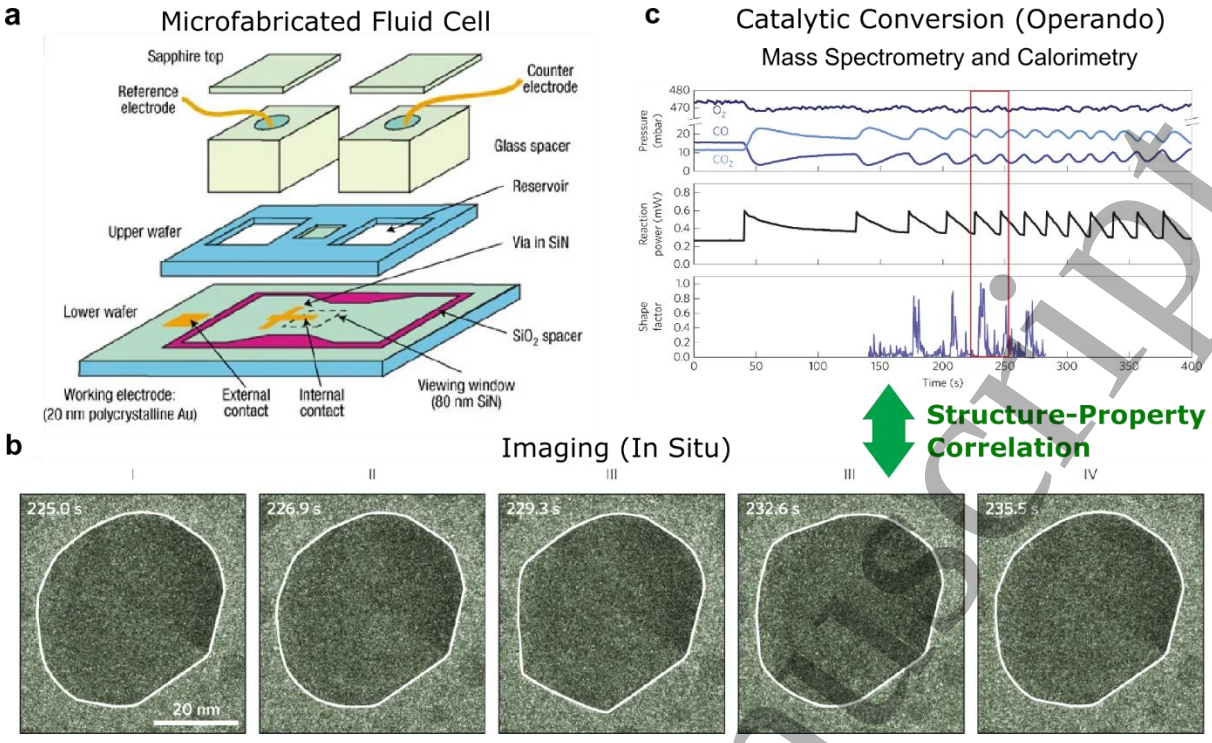


*Figure 1. Development of closed cell platforms for TEM in liquids and gases. (a) Schematic of a microfabricated fluid cell developed by Williamson et al.* [27] *for liquid cell transmission electron microscopy. The samples are encapsulated within a hermetically sealed setup with thin electron transparent silicon nitride membrane windows. In current implementations of this concept, the enclosed environment can be a liquid or a gas at atmospheric pressures. Reprinted with permission from Nature Springer: Nature Materials,* [27], *copyright (2003). (b) Image sequence from* [31] *showing the restructuring dynamics of a Pt NP catalyzing CO oxidation at 386 °C within a 3% CO, 42% $O_2$ and 55% He gas environment. (c) Mass spectrometry data (top) showing an oscillatory behavior in the partial pressures of $O_2$, CO and $CO_2$, calorimetry data (middle) in terms of heater power and shape factor of the Pt NP in (b) as a function of time. Reprinted with permission from Nature Springer: Nature Materials,* [31], *copyright (2014).*

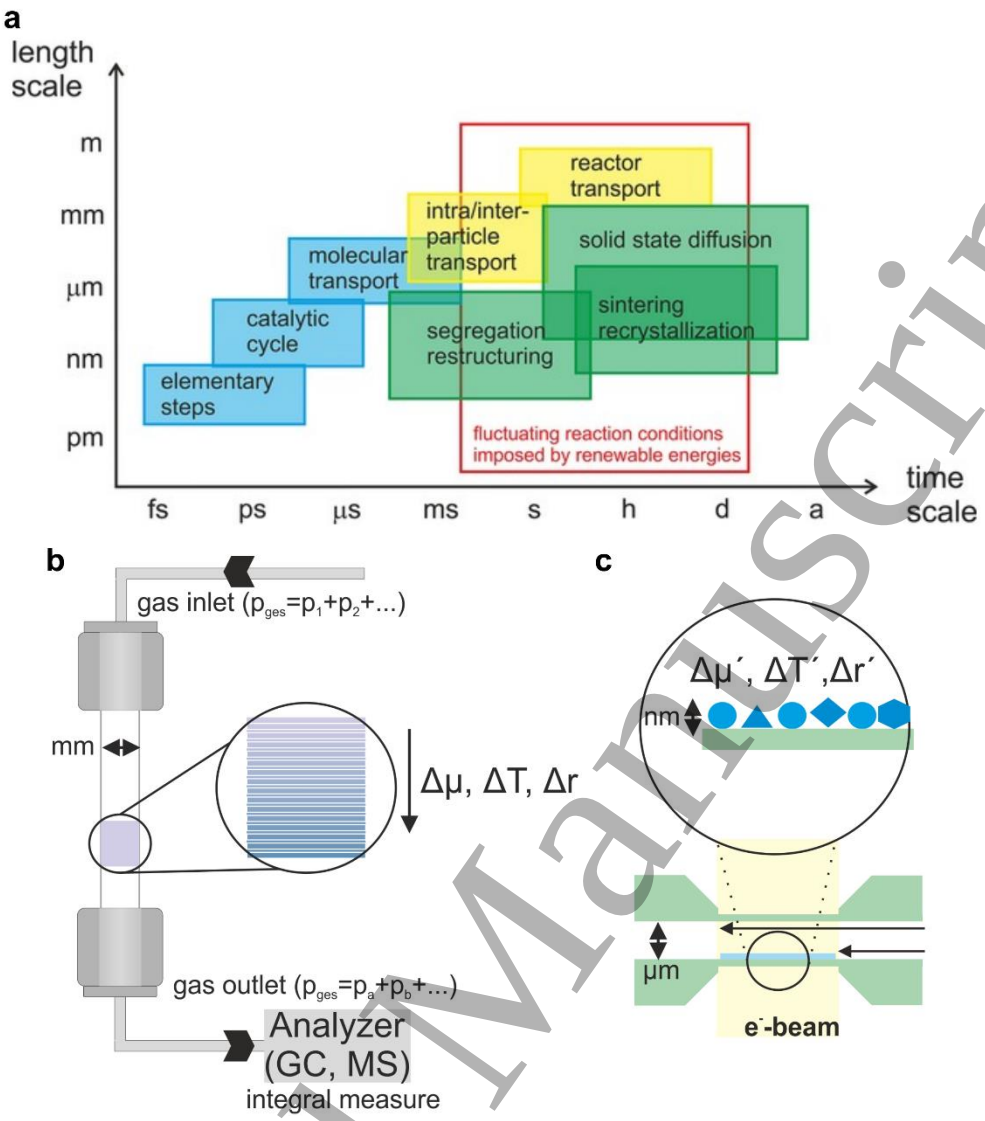


*Figure 2. Length scales in catalytic processes and a comparison of bulk reaction and TEM closed cells. (a) Typical length and time scales of dynamic processes that can take place during catalytic reactions. Reprinted from [19]. © 2017 WILEY-VCH Verlag GmbH & Co. KGaA. Weinheim. Schematics of (b) a plug-flow reactor and (c) closed reaction cell for operando TEM investigations highlighting the range of length scales involved: macroscale (mm), microscale (µm) and nanoscale (nm). The inset in (b) denotes a close-up of a catalytic fixed bed with infinitesimal slabs (white rectangles) along the gas flow direction. The color of the slabs indicates possible differences in the appearance of the catalyst within this area that were induced by a varying local chemical potential (Dµ), temperature (DT), and reactivity (Dr). p denotes the partial pressure of the individual gaseous species, which are different for the inlet and outlet. The analyzer, however, measures an integral quantity averaged over the entire fixed bed. The purple colored slab in (c) denotes the bed of nanoparticles found within the TEM reaction cell. The different length of arrows in (c) emphasizes that a certain quantity of the flowing gas may not directly interact with the nanoscale samples. The inset in (c) shows the differences in local structures of the nanoparticles as well as nanoparticle isolation. Although it is commonly shown how individual NPs are affected by local changes of the chemical potential (Dµ´), temperature (DT´), and reactivity (Dr´), we mention here that the analyzed gas compositions also reflects an integrated quantity.*

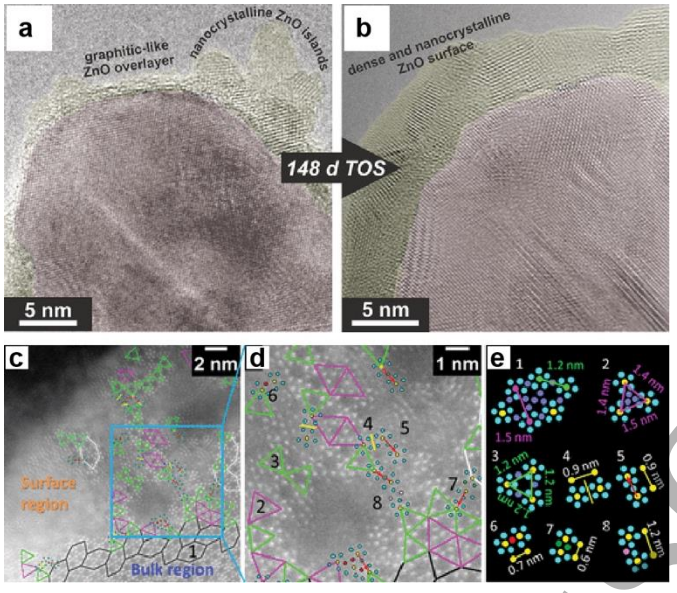


*Figure 3. The complex nature of catalysts. Examples highlighting (a) changes that can take in place in catalysts before and after reaction, and (b) the local inhomogeneities that can occur in the structure of a catalyst. A comparison of Cu/ZnO/$Al_2O_3$ catalysts (a) before and (b) after methanol synthesis. The images show that a dense and nanocrystalline ZnO overlayer layer forms after 148 days time-on-stream. From* [102]. *© 2016 WILEY-VCH Verlag GmbH & Co. KGaA. Weinheim. (c) The HAADF-STEM image show the different local defect motifs found in the surface region of a complex (Mo,V)$O_x$ mixed oxide from* [46]. *(d) Magnified image of a region with the different local motifs. (e) Schematic representation of structural motifs with average distances between central cations of the {(Mo)$Mo_5O_{27}$} units: (1) standard orthorhombic M1 motif, (2, 3) two types of the triangular motifs, (4) mirrored motif, (5) translated motif, (6) shared motif, (7) twinned motif, and (8) rotated motif. Reprinted with permission from* [46], *Copyright 2017 American Chemical Society.*

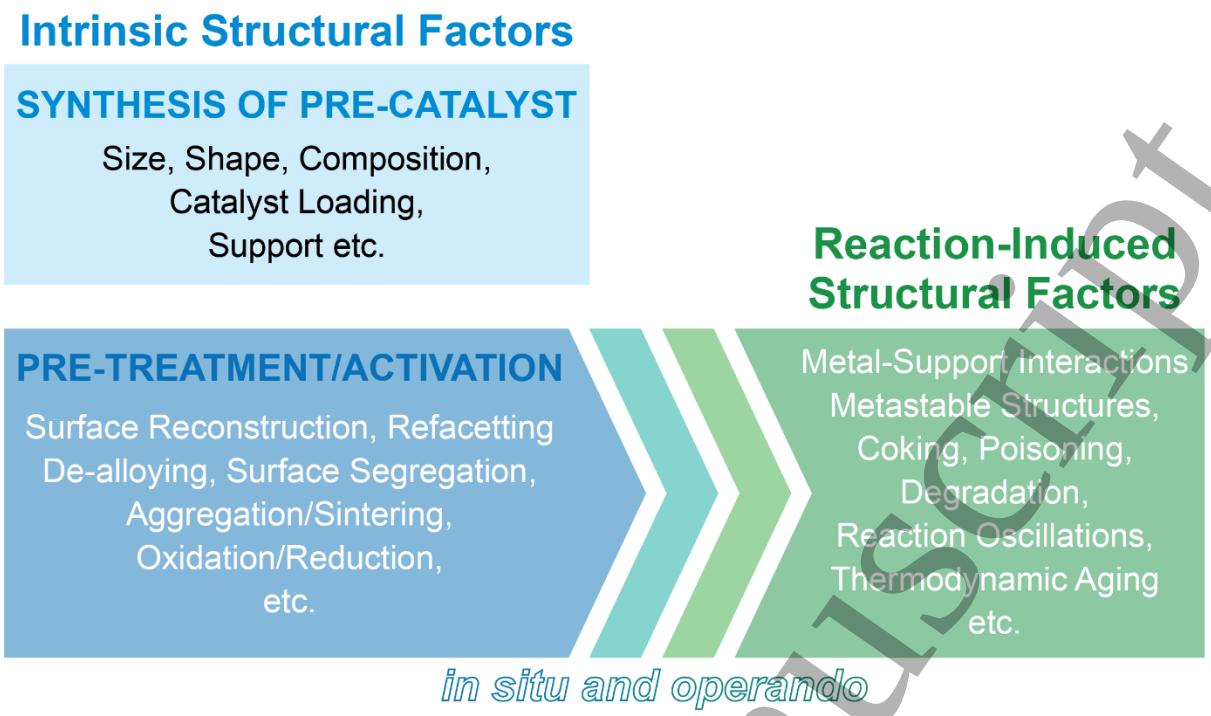


*Figure 4. Examples of intrinsic (blue area) and reaction-induced (green area) structural factors that can impact catalytic performance. The upper box highlights the structural parameters that are largely predetermined by the synthesis protocols. The lower box encompasses the common processes that can be interrogated with in situ or operando EM. Note that the processes described under pre-treatment/activation can undergo further change under reaction conditions and spans both stages.*

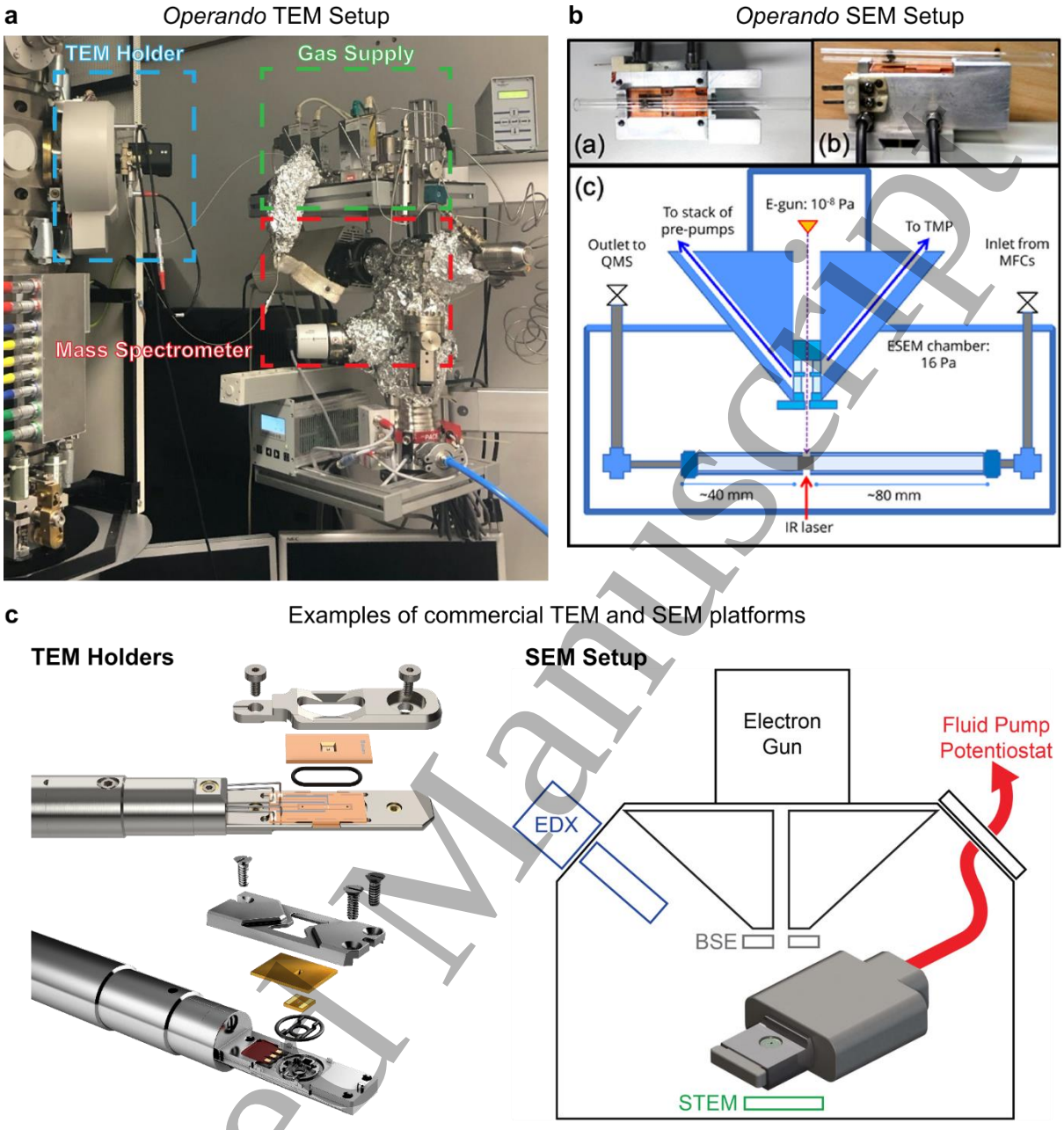


*Figure 5. Examples of in situ and operando SEM/TEM capabilities we have at the FHI. (a) Dedicated TEM for in situ experiments together with a commercial gas flow TEM holder and a home-built gas delivery and mass spectrometry system. From* [100]. *Adapted with permission from Cambridge University Press. (b) Home-built flow reactor for the ESEM. The catalysts are heated with an IR laser. Reprinted from* [159], *Copyright (2020), with permission from Elsevier. (c) Commercial TEM (left) and SEM (right) holders. Images courtesy of DENSsolutions (left-top), Protochips (left-bottom) and Hummingbird Scientific (right).*

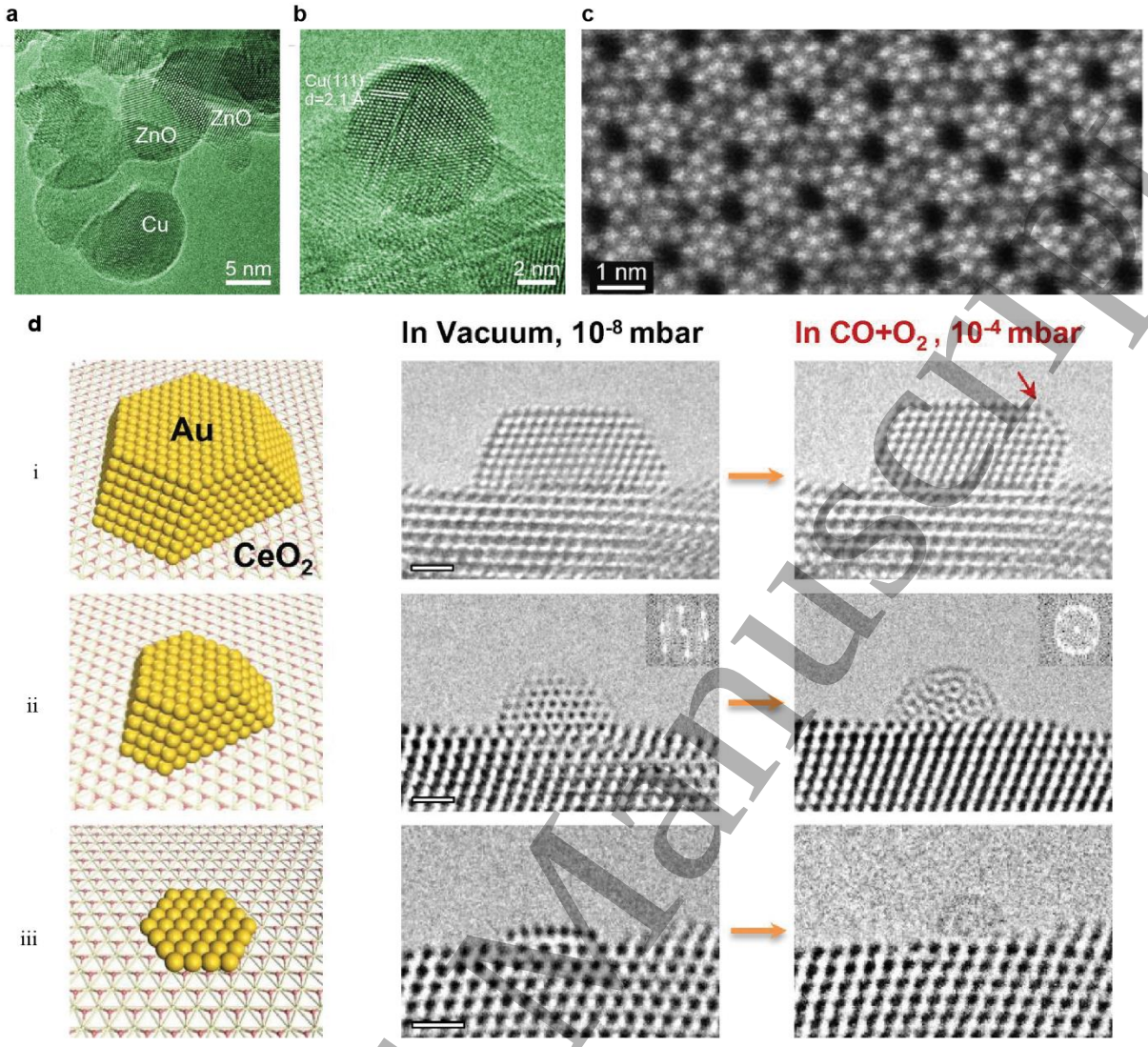


*Figure 6. Examples of ETEM studies looking at catalyst behavior to illustrate the spatial resolution that can be attained under reaction conditions. (a) and (b) show images where industrial-type $Cu/ZnO/Al_2O_3$ catalysts for methanol synthesis are exposed to 1 mbar $H_2$ at 300°C. From* [83]. *Reprinted with permission from AAAS. (c) High resolution STEM image showing the M1 phase of a MoVTe for ethane oxidative dehydrogenation at 350 °C and under 1 mbar of 30% $C_2H_6$, 20% $O_2$ and 50% Ne+He. Adapted from* [239]. *Copyright (2016) American Chemical Society. (d) A Ceria-supported Au NPs of different sizes (i)-(iii) before and after exposure to CO oxidation reaction conditions. Scale bars are 1 nm. From* [240].

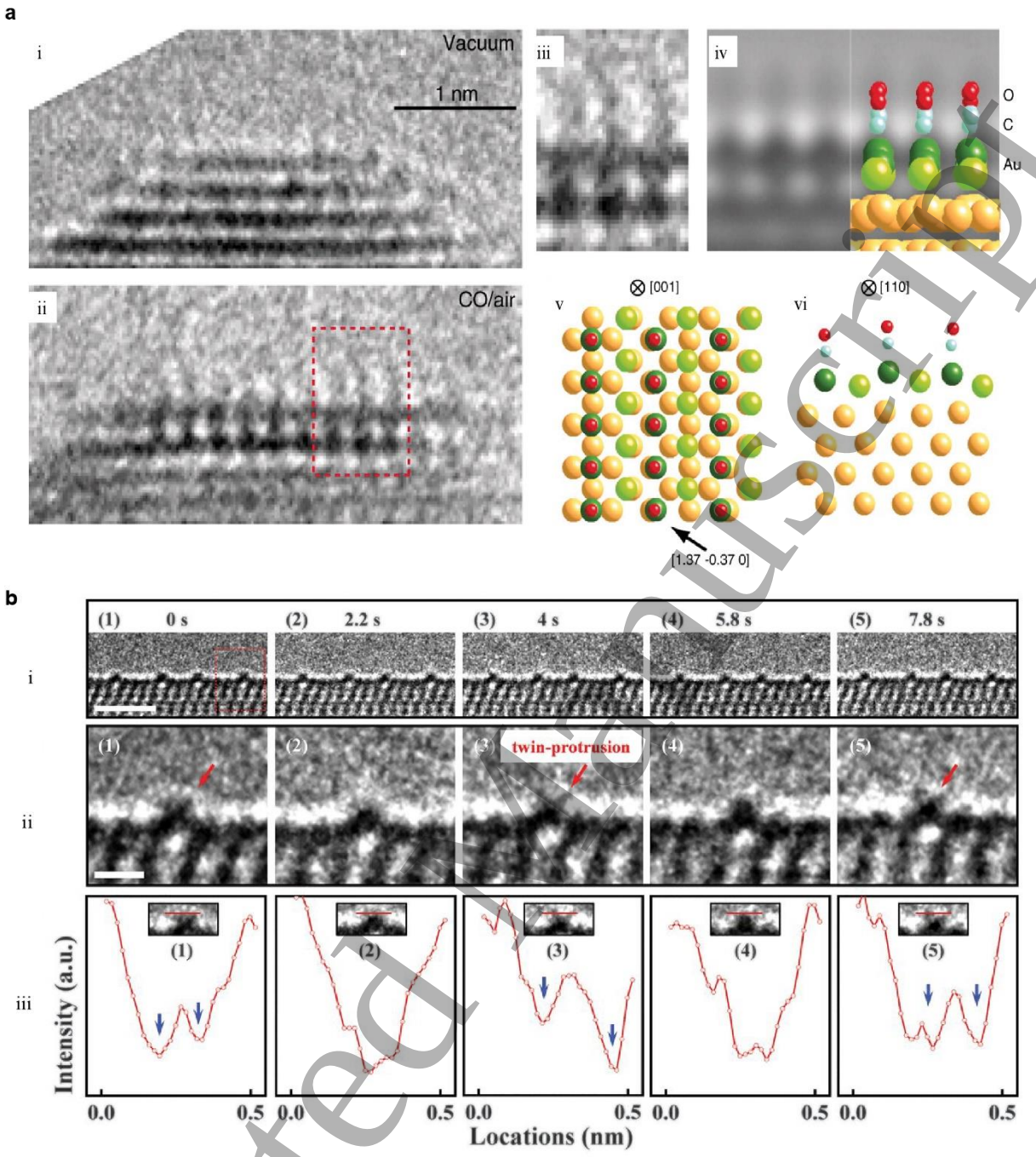


*Figure 7. ETEM studies reporting the observation of adsorbed gas molecules on catalysts under reaction conditions. (a) Comparison of the surface of a Au NP at room temperature (i) under vacuum and (ii) under CO oxidation conditions (1 volume % CO in air at 100 Pa), respectively. Panels (iii) and (iv) compare the image extracted from the red dashed box in (ii) and a simulated image overlaid with a thermodynamic model where blue colored balls are C atoms; red balls are O atoms; darker green balls are Au atoms within the surface hexagonal lattice with adsorbed CO, brighter green balls are the other Au atoms within the surface hexagonal lattice and gold balls are the Au atoms within and below the second topmost surface layer. (v) is a plane view of the model in the [001] direction of crystalline gold and (vi) is a cross-sectional view along the [110] direction of crystalline gold to show the undulating topmost Au layer. From* [199]. *Reprinted with permission from AAAS. (b) (i) Image sequences, (ii) magnified cut-outs and (iii) line profiles extracted from Ref.* [200] *showing a (1 × 4)-(001) $TiO_2$ surface under conditions relevant to the water-gas shift reaction, 5 mbar with 1:1 ratio of CO gas and $H_2O$ vapor and at 700°C) viewed from the [010] direction. The protrusions are attributed*

*to adsorbed water molecules. Scale bars are 2 nm in (i) and 0.5 nm in (ii). From* [200]. *Reprinted with permission from AAAS.*

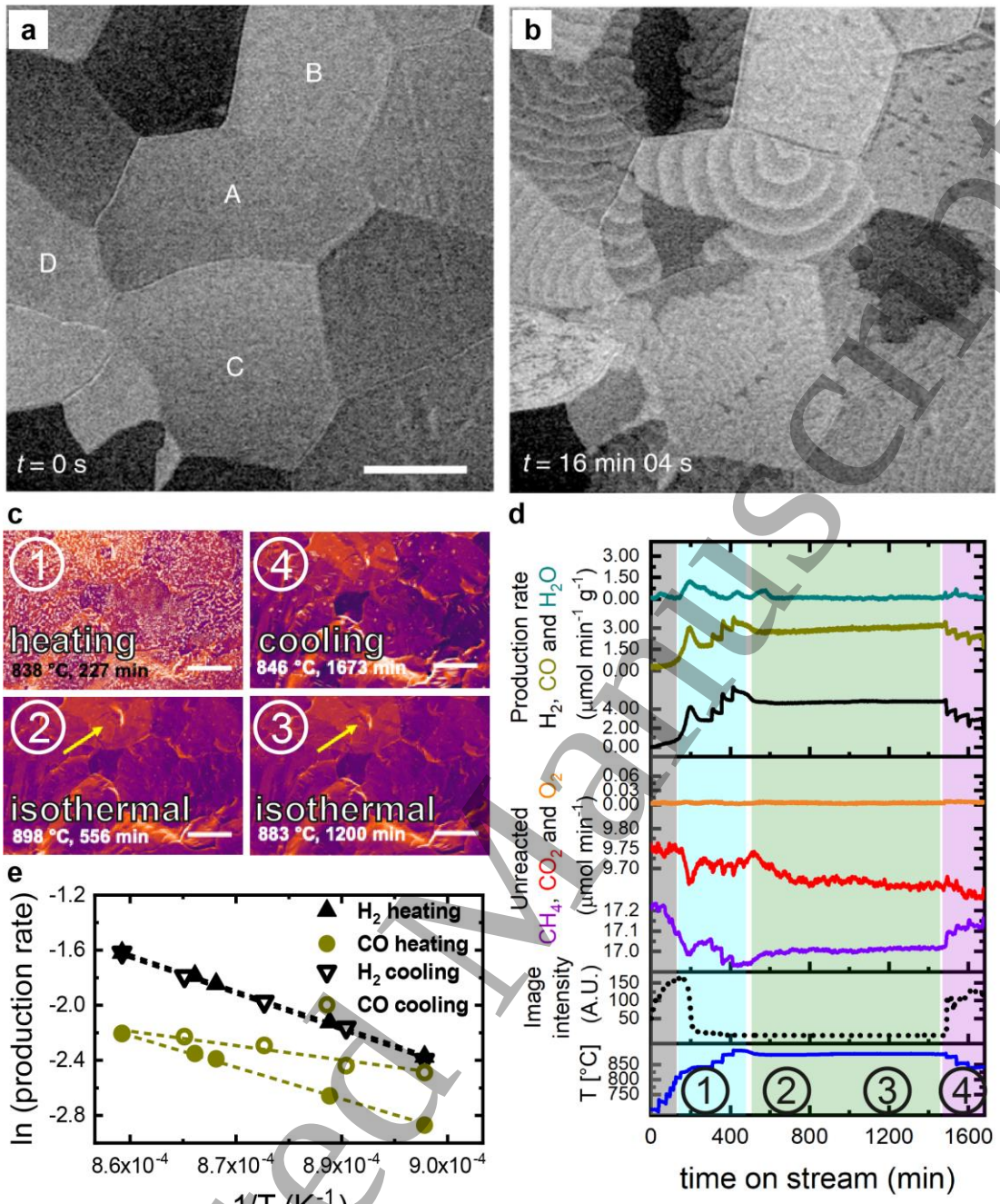

*Figure 8. A sampling of ESEM studies looking at the catalyst behavior under reaction conditions. Comparison of the secondary electron images collected from a platinum foil under $NO_2$ hydrogenation reaction conditions. Images acquired under (a) pure $NO_2$ at $1 \times 10^{-2}$ Pa and (b) 16 mins after $H_2$ was introduced into the gas stream, with T = 175 °C; $pNO_2$:$pH_2$ ≈ 1:10; total pressure = $1 \times 10^{-2}$ Pa. Scale bars are 200 µm. Modified from Ref.* [158] *Reprinted with permission from Nature Springer: Nature Catalysis,* [158]*, copyright (2020). (b) ESEM images recorded under reaction conditions using the operando SEM setup described in Figure 5(b) at selected temperatures and times on-stream under gas flow conditions of 0.3 mLNmin$^{-1}$ Ar; 0.3 mLNmin$^{-1}$ $CO_2$; mLNmin$^{-1}$ $CH_4$. The bright features in (1) and (4) are indicative of surface Ni oxides. (d) Time series showing the reaction traces of $H_2$, CO, $H_2O$, $CH_4$, $CO_2$, and $O_2$, image intensities and the simultaneously recorded temperature of the catalyst. The times corresponding to the images in (c) are indicated. The reaction onset temperature is 806 °C. Reprinted from* [159]*, Copyright (2020), with permission from Elsevier. (e) Arrhenius plots of the catalytic production of $H_2$ and CO. (c)-(e) are adapted from* [159]*. (d) (i) Schematic of an in situ SEM platform adapted from XPS designs using a 100 nm thick silicon nitride membrane as window* [159]*. A comparison of electrochemical SEM observations and XAS measurements obtained from the cell for copper films deposited on the membranes in $CO_2$-saturated 100 mM $KHCO_3$ under (ii)-(iii) open circuit conditions and (iv)-(v) at -1.8 V versus a Ag/AgCl reference. The images indicate a reduction in the size of the deposited copper grains due to the reduction of copper oxide upon the application of the potential as indicated by the (vi) difference image and (vii) difference spectra. Reprinted with permission from* [162]*. Copyright (2020) American Chemical Society.*

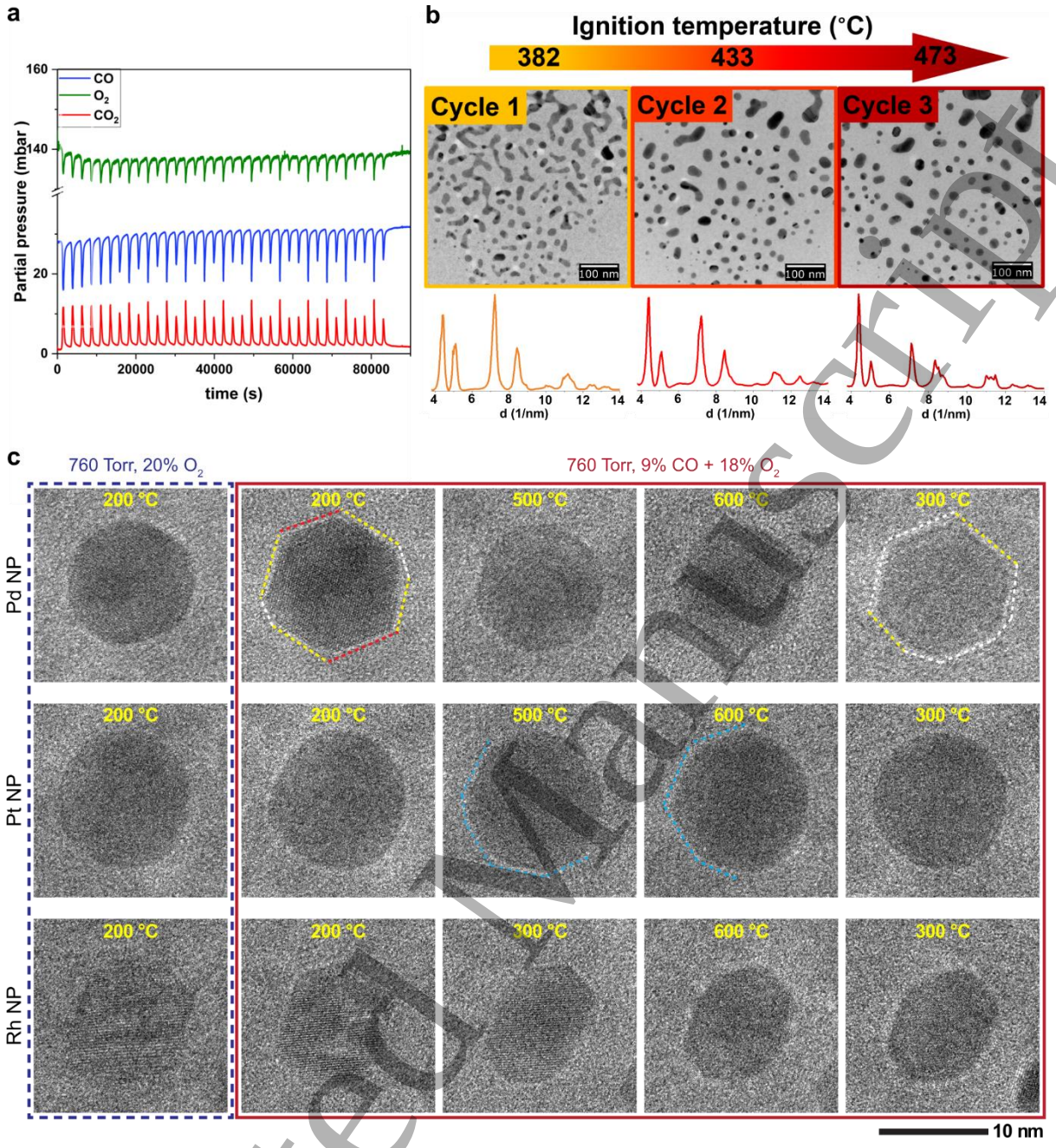


*Figure 9. Operando TEM images of noble metal nanoparticle catalysts during CO oxidation. (a) Changes in the partial pressures of $O_2$ (green), CO (blue) and $CO_2$ measured using an online mass spectrometry during repeated cycling between room temperature and 500 °C under CO oxidation conditions of 700 mbar of 4% CO, 20% $O_2$ and 76% He. From* [100]. *Reprinted with permission from Cambridge University Press. (b) Morphological evolution of Pt NPs during the first three cycles where the temperature was changed from room temperature to 500 °C under the same conditions as (a). It was found that the ignition temperature of the catalysts shifts upwards with each cycle. The line profiles at the bottom describe changes in the radial profiles obtained from the selected area diffraction patterns of the catalysts. Adapted with permission from* [41]. *Copyright (2020) American Chemical Society (c) A comparison of the restructuring observed in Pd, Pt and Rh NPs during CO oxidation in 1 bar of 9% CO 18% $O_2$ and 73% He at different temperatures. The dashed yellow lines in the Pd NP indicate facets that can be indexed to Pd {111}, dashed red lines to Pd {111} and white lines to flat facets that cannot be indexed from the images. The dashed blue lines in Pt NP indicate possible faceting of at the higher temperatures. Reprinted with permission from Nature Springer: Nature Communications,* [51], *copyright (2020).*

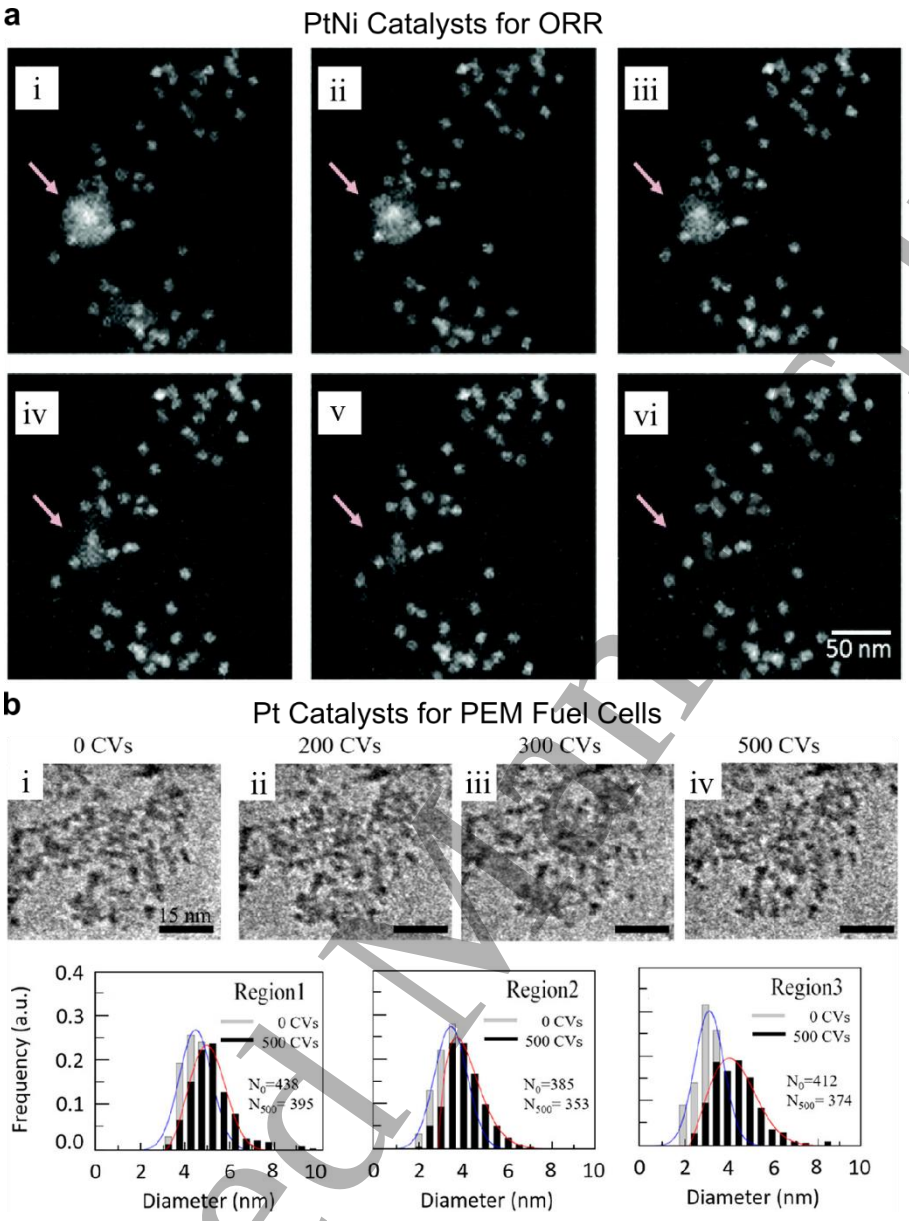


*Figure 10. Examples of electrochemical studies looking at the stability of electrocatalysts during electrochemical cycling. (a) Image sequence describing the dissolution of adventitious Ni during the activation of Pt-Ni alloy fuel cell catalysts with electrochemical potential cycling. The arrow highlights a dissolving Ni particle. From* [95]. *Published by The Royal Society of Chemistry. (b) (i)-(iv) Image sequence (top) showing the changes in commercial Pt NP catalysts for polymer electrolyte membrane fuel cells under repeated electrochemical cycling, i.e. an accelerated stress test, up to 500 cycles. The histograms at the bottom describe the changes in the NP size distribution obtained from different regions that were tracked during the experiment. Reprinted with permission from* [223]. *Copyright (2019) American Chemical Society*

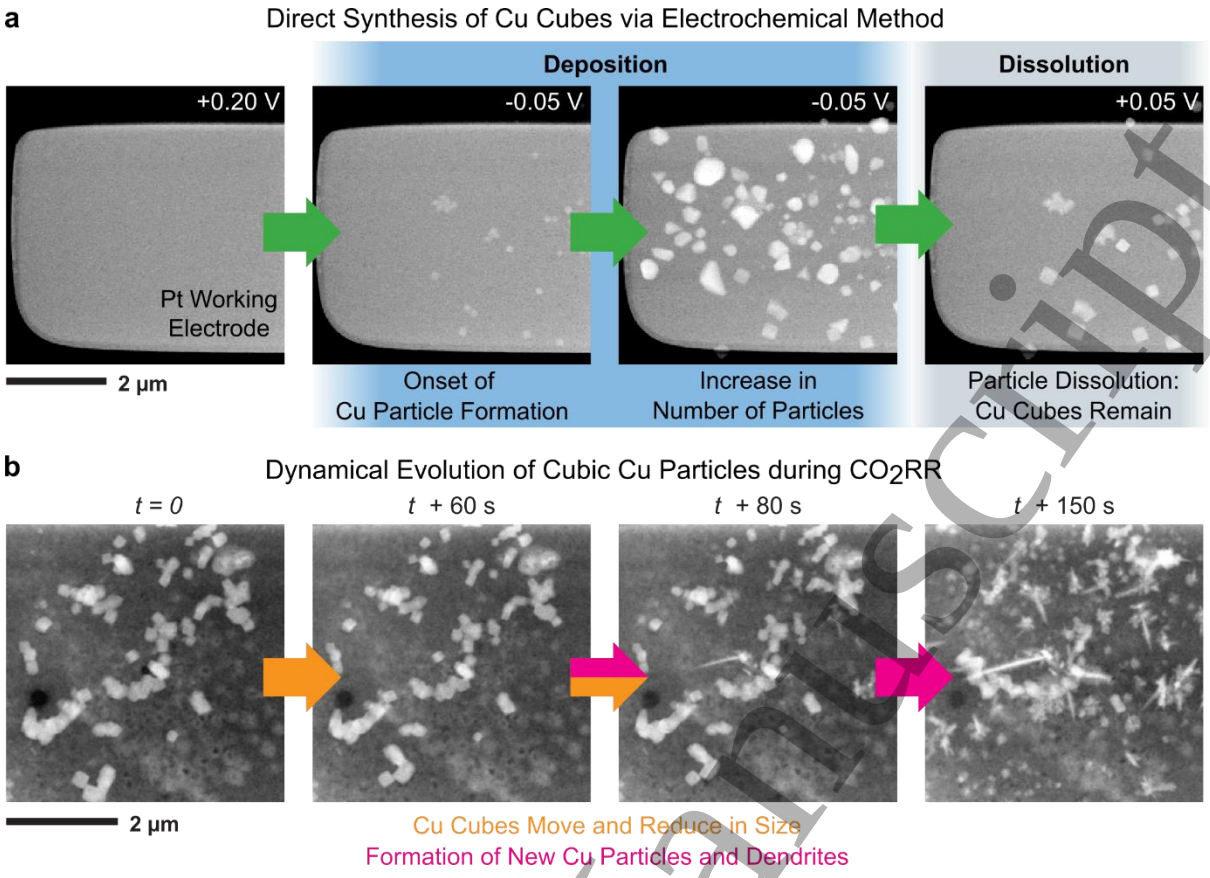


*Figure 11. Electrochemical synthesis of shape-controlled Cu-based catalysts and their subsequent evolution under $CO_2RR$ conditions. (a) Image sequences describing the electrochemical synthesis of $Cu_2O$ cubes from solution. Potential cycling within a narrow window where non-cubic particles dissolve was used. (b) Time-dependent morphological changes in $Cu_2O$ cubes on the working electrode surface after the application of constant -0.7 V potential in $CO_2$-saturated 100 mM $KHCO_3$. The image sequence describes the particle motion, particle size reduction and the formation of new small particles and dendritic structures. The potentials are measured against a pseudo-Pt reference. Data from* [230]. *Adapted with permission from Nature Springer: Nature Communications,* [230], *copyright (2020).*